The Canadian Mineralogist
Vol. 36, pp. 1525-1546 (1998)

A REFINED XRD METHOD FOR THE DETERMINATION OF CHLORITE COMPOSITION AND APPLICATION TO THE McGERRIGLE MOUNTAINS ANCHIZONE IN THE QUEBEC APPALACHIANS

SALAH SHATA[1] AND REINHARD HESSE[2]

Department of Earth and Planetary Sciences, McGill University, 3450 University Street, Montreal, Quebec H3A 2A7

ABSTRACT

Estimation of the heavy atom content in chlorite from XRD measurements has been refined using the intensities of the even-order basal reflections in randomly mounted samples. The distribution of these atoms among octahedral sites is estimated from the intensities of the odd-order basal reflections (003) and (005). The structure-factor calculations were simplified. A newly developed program gives the complete formula of a chlorite and calculates the total iron content (Fe total) in chlorite with a precision of 10%, an improvement over previous studies. The ranges of isomorphic substitution in chlorite based on XRD analyses of this study are comparable to electron microprobe (EMP) results. Chorites from the high-grade diagenetic to very low-grade metamorphic (VLGM) aureole around the McGerrigle Mountains Pluton of Gaspé Peninsula, Quebec Appalachians, are of "ripidolitic" to "pycnochloritic" composition. The [Fe]/[(Fe + Mg)] values of the burial-diagenetic samples are widely scattered, compared to those from the anchizone. During the passage from diagenesis to metamorphism, chlorites lose some Si and at the same time become enriched in Mg, as reflected by increasing [Mg]/[Fe], [(Mg + Al)]/[Fe] and decreasing [Fe]/[(Fe + Mg)] values; thus they approach the ideal trioctahedral structure. The chemical composition of chlorite depends primarily on bulk-rock composition, not on temperature. In the diagenetic realm, the Fe-asymmetry in the octahedral sites decreases with grade, whereas the total iron content [Fe(total)] increases, possibly reflecting preferential incorporation of Fe in the brucite-like sheet. With advancing VLGM conditions, on the other hand, decreasing [Fe(total)] in the octahedral sites is coupled with increasing Fe-asymmetry, possibly due to [Fe] decrease in the brucite-like sheet preferentially over the talc-like layer. Chlorite composition and crystallinity are highly correlated. Both composition and crystallinity index are a function of grain size, especially in burial-diagenetic samples. Structurally, both Ib and IIB chlorite polytypes have been identified. Swelling chlorites are absent, on the basis of XRD patterns of ethylene-glycol-solvated samples. The distribution of chlorite polytypes is also correlated with chlorite crystallinity and grain size.

Keywords: chlorite, composition, formula, Fe-asymmetry, crystallinity, burial diagenesis, anchizone, McGerrigle Mountains pluton, Quebec Appalachians.

SOMMAIRE

Nous avons affiné la façon d'évaluer la teneur en atomes lourds d'une chlorite par diffraction X en utilisant l'intensité des réflexions fondamentales d'ordre impair dans des échantillons non orientés. La distribution de ces atomes parmi les sites octaédriques repose sur les intensités relatives des réflexions (003) et (005). Nous avons simplifié le calcul des facteurs de structures. Un nouveau logiciel permet de déterminer la formule chimique complète d'une chlorite, et sa teneur en fer total, avec une précision de 10%, ce qui constitue une amélioration par rapport aux études antérieures. Les intervalles de substitution isomorphique dans une chlorite déterminés par analyse diffractométrique sont comparables à ceux que l'on établit avec une microsonde électronique. Les chlorites d'origine diagénétique avancée ou à degré de métamorphisme très faible qui se trouvent dans l'auréole de contact du pluton des monts McGerrigle, dans les Appalaches du Québec, auraient une filiation "ripidolitique" à "pycnochloritique". Les valeurs [Fe]/[(Fe + Mg)] des échantillons sujets à la diagenèse lors de l'enfouissement sont éparses, en comparaison de celles de l'anchizone. Au cours du passage de la diagenèse au métamorphisme, la chlorite perd une partie de son Si et en même temps devient plus fortement magnésienne, comme le témoignent [Mg]/[Fe], [(Mg + Al)]/[Fe], qui augmentent, et [Fe]/[Fe + Mg)], qui diminue. La chlorite devient donc davantage trioctaédrique. La composition chimique d'une chlorite dépend surtout de la composition globale et non de la température. Dans l'intervalle de la diagenèse, l'asymétrie dans la distribution du Fe dans les sites octaédriques diminue ave l'intensité de la recristallisation, tandis que la teneur en fer total augmente, question de préférence du Fe pour le feuillet de type brucite. A mesure qu'augmente l'intensité du métamorphisme, par contre, la diminution du fer total dans les sites octaédriques est couplée avec l'augmentation dans l'asymétrie de la distribution du fer, peut-être un résultat de la diminution du Fe dans le feuillet de type brucite par rapport à la proportion dans le feuillet à caractère de talc. La

[1] *E-mail address*: shata@geosci.lan. mcgill.ca, salah215@hotmail.com
[2] *E-mail address*: rein_h@geosci.lan.mcgill.ca, reinhard.hesse@ruhr-uni-bochum.de

composition et la cristallinité d'une chlorite sont fortement liées. Les deux paramètres dépendent de la granulométrie, surtout dans les échantillons diagénétiques enfouis. Du point de vue structural, les deux polytypes de la chlorite, Ib et IIb, ont été identifiés. Par contre, les chlorites gonflantes semblent absentes, comme l'indiquent les échantillons traités au glycol d'éthylène. La distribution des polytypes montre aussi une corrélation avec la cristallinité et la granulométrie.

(Traduit par la Rédaction)

Mots-clés: chlorite, composition, formule, asymétrie dans la distribution du Fe, cristallinité, diagenèse d'enfouissement, anchizone, pluton des monts McGerrigle, Appalaches, Québec.

Introduction

Chlorites, ubiquitous phyllosilicates in sedimentary, metamorphic and hydrothermal environments, display a high degree of isomorphous substitution. Their chemical compositions, and especially the ratios Si/Al, [Fe(total)]/[(Fe^{2+} + Mg)] and [(Fe^{2+} + Mg)]/[Al], are known to be a function of the physicochemical conditions of crystallization and the bulk composition of the host rocks (Cathelineau & Nieva 1985, Walshe 1986, Cathelineau 1988, Laird 1988, Hillier & Velde 1991, Prieto *et al.* 1991, Spötl *et al.* 1994, Xie *et al.* 1997).

The exact determination of the chemical composition of chlorites is a challenging task for a variety of reasons: i) the difficulty in preparing pure samples of chlorite for wet-chemical analysis, ii) the fine to very fine grain-size, the inequant shape of grains and their intimate intergrowth with other phyllosilicates (*e.g.*, white mica; Ahn & Peacor 1985), iii) the uncertainty in determining the ratio Fe^{2+}/Fe^{3+} (Nieto 1997), (iv) the possibility of a transitional state between trioctahedral and dioctahedral chlorites, and (v) the complexity of isomorphic substitutions. In spite of these drawbacks, the electron microprobe (EMP) is widely used to analyze chlorite in coarse-grained samples, but is poorly adapted to the analysis of fine-grained materials (Árkai 1991). Thus, the development of X-ray methods for estimating the composition of chlorite species in fine-grained materials has become necessary. The relationship between the chemical composition of chlorite and cell dimensions [d(001) and d(060)], and the relative intensities of selected basal reflections in the X-ray-diffraction (XRD) pattern, have been the subject of previous studies by Brindley (1961), Brindley & Gillery (1956), Petruk (1959), Schoen (1962), Bailey (1972), Brindley & Brown (1980), Walker *et al.* (1988), Moore & Reynolds (1997), and Rausell-Colom *et al.* (1991). These methods give [^{IV}Al] and [Fe^{2+}] only, with various degrees of precision.

The aim of the present study was to establish a simple, rapid, and precise method to deduce the chemical composition of chlorite from XRD measurements. This method has been applied to trace the chemical changes in diagenetic and anchizonal chlorite from Cambro-Ordovician shales and slates surrounding the McGerrigle Mountains pluton in the Gaspé Peninsula of the Quebec Appalachians. The ultimate aim of this investigation is to trace the chemical changes during high-grade diagenesis and very low-grade metamorphism (VLGM) in this area.

Methods and Materials

The X-ray-diffraction analysis was carried out on a 12 kW Rigaku D/Max 2400 automated powder diffractometer with a rotating copper anode. Operating conditions were 40 kV and 120 mA. The diffractometer was equipped with a secondary monochromator and a theta-compensating slit-assembly. Two grams of freeze-dried chlorite powder were placed in sample holders by the back-filling technique of Moore & Reynolds (1997), in order to keep preferred orientation at a minimum. Samples were scanned with step size of 0.01° 2θ per second and a time constant of 1 second. Samples were scanned with a computer-controlled software system (Reg-Meas DF–310D), and the data were collected with the Jade Plus software. The theta-compensating slit-assembly maintains the area irradiated by X-rays constant for any 2θ.

According to Walker *et al.* (1988), sample thickness, sample length, and preferred orientation have to be taken into consideration in order to avoid spurious results from XRD data. Because the odd-order reflections are weak and may be undetectable from randomly oriented powders, every possible effort has to be made to increase the concentration of chlorite in powdered samples, *e.g.*, by isomagnetic separation. In order to improve the precision of the basal reflection measurements d(00l), quartz, the mineral most commonly accompanying chlorite, is used as an internal standard. However, the presence of other phases such as kaolinite or serpentinite may hinder quantification by the X-ray method (Ryan & Reynolds 1997).

Fifteen samples from the Lower Paleozoic sedimentary sequences of high-grade diagenesis to very low-grade metamorphism from the Gaspé Peninsula of the Quebec Appalachians were studied with the methods outlined above. Eight samples are from burial diagenetic environments; the remaining seven are from the anchizonal aureole around the Devonian McGerrigle Mountains pluton (Fig. 1). Detailed locations of samples and geology of the study area will be given in the first author's thesis (in prep.).

Seventeen samples from the Phelps Dodge massive sulfide deposit in Matagami, Quebec, were provided by

W.H. MacLean as reference samples. Details of sample locations and geology are given in Kranidiotis & MacLean (1987).

Structure and Crystal Chemistry of Chlorite-Group Minerals

The chlorite structure ideally consists of negatively charged 2:1 layers ("talc-like layers") bonded together by positively charged interlayer sheets of octahedra ("brucite-like sheets"; Bailey 1988a) (Fig. 2). As Si is replaced by Al ($Si_{8-x}Al_x$), the 2:1 layer acquires a negative charge $-x$, which is balanced by a corresponding replacement of divalent cations by trivalent cations in the octahedrally coordinated sites of the brucite-like sheet. One of the most common cationic substitutions in chlorites is of the type $^{VI}Mg^{IV}Si \rightleftharpoons {}^{VI}Al^{IV}Al$, known as the "Tschermak exchange". This substitution leads to a redistribution of the charge between tetrahedral and octahedral sheets, but maintains overall charge-balance. Although the most common octahedrally coordinated cations in chlorite are Mg^{2+}, Fe^{2+}, and Fe^{3+}, there is a considerable range of cationic substitution. The great majority of chlorites are trioctahedral in both the brucite-like sheet and the 2:1 layer octahedral sheet. The present study focuses on such tri-trioctahedral chlorites, which, for simplicity, are simply called trioctahedral chlorites.

Estimation of the Chemical Composition of Chlorite Using XRD Data

Three different approaches have been established previously to estimate the chemical composition of chlorite-group minerals using XRD data: the basal-reflection spacing measured at low-2θ angles, the b cell parameter, and X-ray intensities of basal reflections at low-2θ angles.

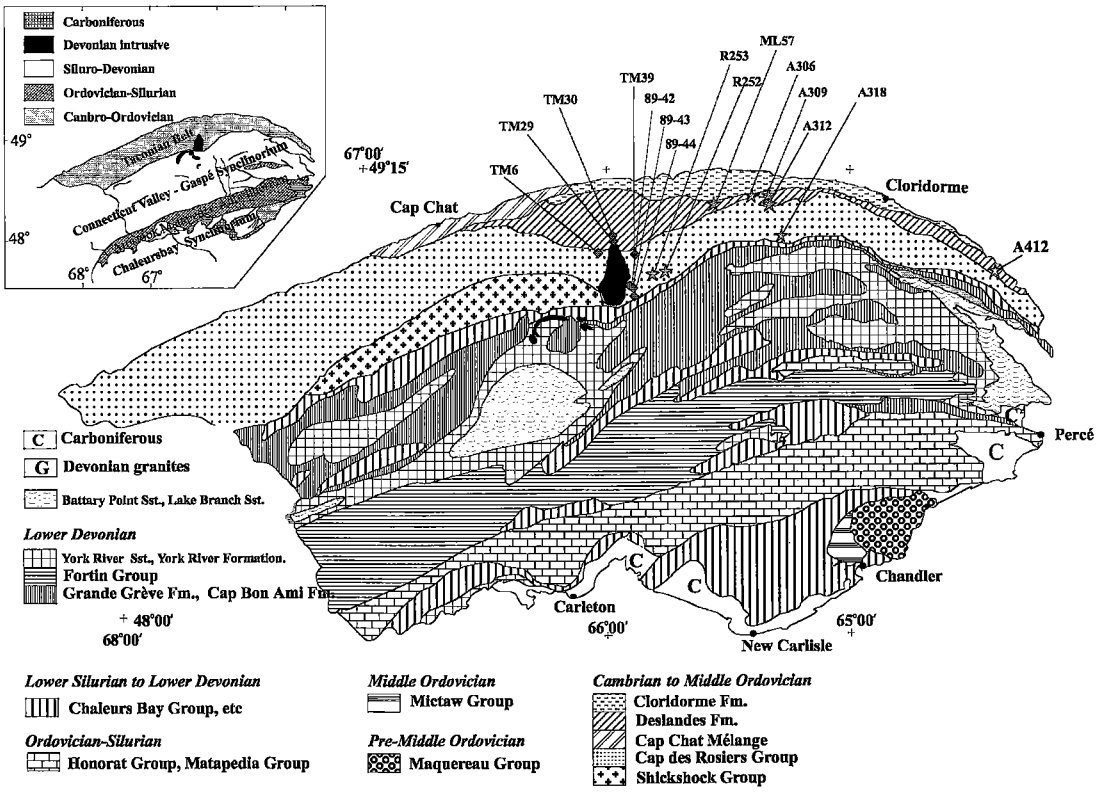

FIG. 1. Geological map of Gaspé Peninsula (after Skidmore & McGerrigle 1967), showing the main stratigraphic units, structural elements and sample localities. Open stars: burial-diagenetic samples and VLGM samples; closed diamonds: McGerrigle anchizone. The dominant Devonian intrusive body is the McGerrigle Mountains pluton. Adapted from Hesse & Dalton (1991).

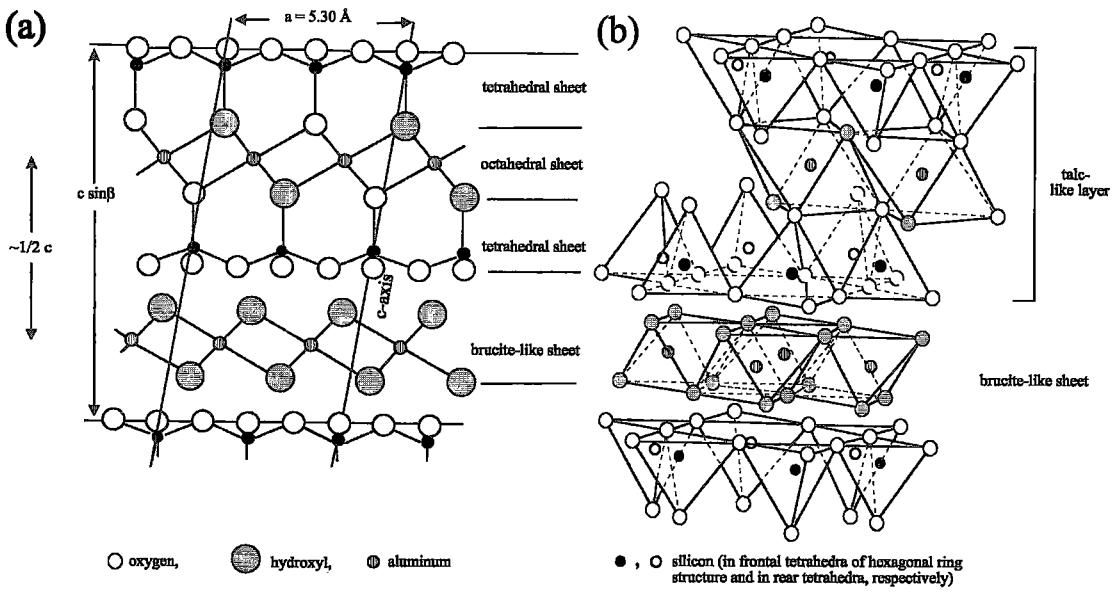

FIG. 2. The chlorite structure. (a) Projection of chlorite structure on the *ac* plane. (b) Diagrammatic sketch of chlorite structure. Modified after Grim (1968).

Estimation of [^{IV}Al] and [^{VI}Al] from the d-value of the basal reflections

The basal spacing of a chlorite depends on its composition and the bonding between sheets of tetrahedra and octahedra. Gruner (1944) and Bannister & Whittard (1945) first correlated the basal spacing with the extent of replacement of Si by Al, and attributed the variation of $d(001)$ mainly to variations in strength of ionic bonds (Brindley & Gillery 1956). Increasing substitutions in both the tetrahedral and octahedral sheets tend to increase the ionic attraction between the 2:1 layer and the brucite-like sheet and, consequently, to decrease the layer thickness measured by the d-value of the basal reflection, $d(001) = c \sin\beta$, where c is the periodicity in the Z direction, and β is the angle between the X and Z axes. Thus the value of the layer charge x may be estimated from basal-spacing measurements (Bailey 1972, Brindley & Brown 1980).

Despite discrepancies among equations in the literature, the use of the $d(001)$ graph or regression equation gives reasonable estimates of ^{IV}Al for most trioctahedral chlorites (Bailey 1972, 1975, Whittle 1986). As these equations were derived for trioctahedral chlorites, they should not be applied to dioctahedral species. Since chlorites have a well-defined layer structure parallel to basal reflections ($00l$), these reflections will provide the clearest, most precise information on the distribution of cations.

In the present study, reference samples of coarse-grained chlorite from the Phelps Dodge deposit were used to establish a correlation between the chemical composition based on electron-microprobe data and the $d(003)$ and $d(005)$ values in order to calculate [Si] (eq. 1) and [(total) Al] (eq. 2), respectively. Also, the reference samples were used to check the validity of the correlation factors for the linear relationships of [Si] and [(total) Al] with $d(003)$ and $d(005)$. The factors are 0.74 and –0.79, respectively.

$$[Si] = 0.632*d(003) - 92.142 \quad \text{(eq. 1)}$$

$$[Al(total)] = -100.679*d(005) + 290.618 \quad \text{(eq. 2)}$$

The [^{IV}Al] is calculated as 8 – [Si], and [^{VI}Al] = [(total)Al] – [^{IV}Al]. Structural balance in chlorite requires that the brucite-like sheet have a positive charge equivalent to the negative charge of the talc-like layer. To obtain a positive charge, a certain minimum number of trivalent cations must occur in octahedrally coordinated positions. In case of paucity of [^{VI}Al], other trivalent octahedrally coordinated cations (*e.g.*, Fe^{3+}) are present. Foster (1962) discussed the variability in the relationship between [^{IV}Al] and [^{VI}Al] in chlorites as follows, the same principles being used for calculation of the chlorite formula:

(i) In few chlorites, the [^{VI}Al] is equal to [^{IV}Al], with R^{2+} (Mg, Fe^{2+}) occupying the rest of the octahedrally coordinated positions, so that the octahedral occupancy (Σ^{VI}) is close to the maximum value of 6.00 atoms per formula unit (*apfu*). In theory, replacement of Si^{4+} by

Al^{3+} *via* the Tschermak exchange implies an equivalent amount of octahedral replacement of R^{2+} by Al^{3+} in order to maintain charge balance. Therefore, [^{IV}Al] should equal [^{VI}Al], although in natural chlorites this is rarely the case (Foster 1962).

(ii) If [^{VI}Al] is in excess of [^{IV}Al] plus any other trivalent cation in the tetrahedrally coordinated position, such as Fe^{3+}, then the excess ^{VI}Al may be interpreted as replacing R^{2+} cations in a 2:3 ratio, and octahedral-site occupancy becomes deficient by an equivalent amount. In other words, the total number of cations in the octahedral sheets does not reach 6 (per one half-unit cell), and the value (6 – "total number of cations in the octahedral sheet") equals the number of vacancies. The vacancies in the octahedral sites are always equal to one-half the number of trivalent octahedrally coordinated cations in excess of tetrahedrally coordinated trivalent cations.

(iii) In other chlorites, [^{VI}Al] is less than [^{IV}Al]; some other trivalent cation, usually Fe^{3+}, is required for structural balance. The Fe^{3+} is assumed to replace ^{VI}Al in a 1:1 ratio. This is supported by the octahedral occupancy, which is 6.00 *apfu* or very close to it.

Calculation of total Fe content using the cell parameter b

There are two different approaches to estimate the [Fe(total)] in chlorite from XRD data. According to Whittle (1986), the *d*(060) reflection can be used to estimate [Fe^{2+}] in the octahedral sheet. The relationship between the periodicity along *b* in trioctahedral chlorites and chemical composition is $b = 9.23 + 0.03[Fe^{2+}] \pm 0.0285$ (Radoslovich 1962). The *b* parameter is best determined from 6*d*(060) for monoclinic chlorites. Nieto (1997) compared the proportion of heavy atom (Fe) determined from basal reflections with electron-microprobe data for chlorite in metapelites, and pointed out the uncertainty in relating intensities to structural factors owing to differences in the diffractometer geometry and methods of sample preparation. Nieto (1997) reaffirmed the use of the *b* parameter to estimate [Fe(total)], and proposed a simplification of the Rausell-Colom *et al.* (1991) equation: $d(001) = 14.359 - 0.0905[^{VI}Al] - 0.035[^{IV}Al] - 0.0201[Fe^{2+}] + 0.0938[Cr^{3+}] + 0.028[Mn^{2+}] - 0.059[Li^{+}]$. Nieto established the proportion of the cations other than Fe in both the octahedral and tetrahedral sheets by making the following assumptions: no Fe^{3+}, $\Sigma^{VI} = 5.9$, $^{VI}Al = {}^{IV}Al + 0.2$; he provided no justification for these simplifying assumptions.

Is the b parameter valid as an estimator of total Fe?

The *b* parameter reflects all substitutions. Since ^{IV}Al has a significantly larger ionic radius (0.39 Å) than Si (0.26 Å), increasing replacement of Si by Al tends to expand the tetrahedral sheet. Also, if Mg ions are regarded as normal octahedrally coordinated cations, then replacement of Mg^{2+} (r = 0.72 Å) by Al^{3+} and Fe^{3+} (0.53 and 0.64 Å, respectively) tends to shrink the sheet, whereas replacement by Fe^{2+} ions (0.78 Å) tends to expand the sheet; all ionic radii from Shannon & Prewitt (1969, 1970). However, the overall contribution of the expansion of tetrahedra due to increasing replacement of Si by Al, and that of the contraction of octahedra due to replacement of Mg by Fe^{3+} is very small; the resultant value of the *b* parameter seems to be determined principally by the extent of Fe^{2+} substitution for Mg (Brindley & Gillery 1956). Hey (1954), Bailey (1975, 1988a, b), Shirozu (1980), Whittle (1986), and Ebina *et al.* (1997) demonstrated the asymmetry of the Al distribution between tetrahedrally and octahedrally coordinated sites. Therefore, the proposed overall contribution to an expansion (in tetrahedral sheets) or contraction (in octahedral sheets) due to incorporation of Al may be important. The resultant *b* parameter thus depends not only on the amount of Fe^{2+} present, but also on other cationic substitutions. The lack of information (or at best uncertainty) about the ratio Fe^{2+}/Fe^{3+} is another source of error. In conclusion, the *b* parameter cannot be used for a reliable determination of chlorite species.

Estimation of the proportion of heavy atoms [Fe] using the relative intensities of the basal reflections

X-ray diffraction of the basal planes of chlorite can be interpreted as reflections from the octahedral and tetrahedral sheets. The intensity of the diffracted beam is a measure of the scattering power of the atoms in those sheets. Methods to estimate chlorite composition make use of the greater scattering factors for Fe, Mn, Cr, and Ni relative to Mg and Al, as recorded by the X-ray intensities of basal reflections at low-2θ angles. The methods used to estimate the structural factor (amplitude) from the measured relative intensities of certain basal reflections give not only the total heavy metal content in the octahedrally coordinated sites, designated *Y*, but also approximate values for the asymmetry (*D*) in the distribution of heavy atoms between the octahedral sheet in the 2:1 layer and the interlayer brucite-like sheet. Brindley & Brown (1980) and Chagnon & Desjardins (1991) defined the asymmetry as *D* = Fe(sil) – Fe(hyd), where Fe(sil) is the Fe content in the talc-like layer, and Fe(hyd) is the Fe content in the interlayer brucite-like sheet.

The maximum and minimum values of *D* are +6 and –6, respectively; values of *Y* vary from 0 to 12. Both *Y* and *D* are based on a chlorite formula that contains a total of 12 cations in the two types of octahedral sites and whose formula can be written as

talc-like layer	$[Mg_{6-a-x2}\ Fe^{2+}{}_{a}\ (Si_{8-x}Al_x)\ O_{20}\ (OH)_4]^{-x+x2}$
brucite-like sheet	$[Mg_{6-b-x1}\ Fe^{2+}{}_{b}\ Fe^{3+}{}_{x2}\ Al_{x1}\ (OH)_{12}]^{+x1}$
chlorite composition	$[Mg_{12-a-b-x}\ Fe^{2+}{}_{a+b}\ Fe^{3+}{}_{x2}\ Al_{x1}\ (Si_{8-x}Al_x)\ O_{20}(OH)_{16}]$

where $x = x1 + x2 = [^{IV}Al]$, which varies from 1.6 to 3.2 in most chlorites (Brindley & Brown 1980, p. 341).

Theoretical background

Because the two octahedral sheets of chlorite are separated by $c/2$ along the Z direction (Fig. 2), the contributions of the heavy atoms (Fe) to scattering are in phase for even orders of (00l), and out of phase for odd orders.

Where there is a symmetrical distribution of cations in the octahedral sheets, the only contribution to the odd orders comes from the network of hexagonal Si–O rings, because the contributions from cations in both octahedral sites cancel each other. An asymmetrical distribution of octahedrally coordinated cations between the talc-like layer and brucite-like sheet, on the other hand, has a pronounced effect on the odd-order reflections because the contributions from the octahedral sheets no longer cancel out completely, thus adding to the contribution from the hexagonal network of Si–O tetrahedra. This is the basis for using the XRD intensity of the relatively weak odd-order basal reflections (001), (003), and (005), to characterize the distribution of Fe in the two types of octahedral sites of chlorite.

Intensities of X-rays diffracted from even-order basal reflections are strong because the scattering from octahedral sheets is in phase and thus reinforced. The even-order basal reflections remain unaffected by Fe-asymmetry. Their intensity is proportional to the occupancy by the sum of the atoms of Fe + Mn + Cr in the octahedra (Fig. 2); the scattering power of these atoms is about twice that of the light atoms (Mg, Al, and Si).

Characteristics of XRD Patterns of Chlorite

From the intensity ratio of X-rays diffracted from the odd-order reflections, the distribution of the light and heavy atoms in the two octahedral sheets in a chlorite can be determined. In the case of an asymmetrical distribution of Fe in a trioctahedral chlorite, with Fe-enrichment in octahedral sites of the talc-like layer over those of the brucite-like sheet, the intensity of the (001) and (005) reflections increases relative to the (003) reflection. Enrichment of Fe in the brucite-like sheet produces weak intensities of (001) and (005) relative to (003).

The intensities $I(003)$ and $I(005)$ can be used with confidence, whereas $I(001)$ is unreliable, as it is a low-angle reflection. In the present study, the relationship between the ratio of the structural amplitude factors $[F(003)/F(005)]$ and Fe-asymmetry is calculated and plotted (Fig. 3). The structure factors $F(003)/F(005)$ are calculated from the relative intensities of these particular reflections (details of the calculation are discussed below and in the Appendix). From the logarithmic relationship in Figure 3, the Fe-asymmetry is obtained.

Symmetrical distribution

As mentioned earlier, the intensity of the even-order basal reflections increases in proportion to the occu-

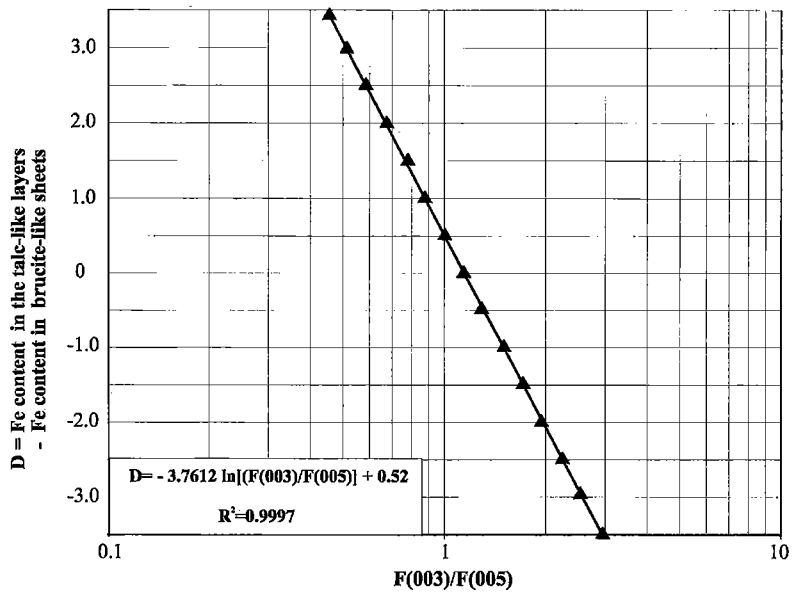

FIG. 3. Determination of Fe distribution (asymmetry) in the octahedral sites of chlorites using structure-factor ratios.

pancy of heavy atoms in octahedral sites (Brindley & Gillery 1956). The intensity of the odd-order basal reflections is independent of the proportion of total heavy atoms in octahedral sites. Consequently, the ratio $[I(002) + I(004)]/I(003)$ should provide a good estimate of the total heavy atom (Fe) content in octahedrally coordinated sites (Fig. 4).

Asymmetrical distribution

In cases where the two types of octahedral sheets contain unequal proportions of heavy atoms, the intensity of the even-order basal reflections is still proportional to the total number of heavy atoms in octahedrally coordinated sites (equal to those in "symmetrical" chlorite), but the odd-order reflections will be different from those in "symmetrical" chlorite. In the ratio $[I(002) + I(004)]/I(003)$, the $I(003)$ has to be corrected for asymmetry before the ratio can be used to estimate the total proportion of heavy cations in octahedral sites (Petruk 1964). The correction factor for the odd-order reflection can be deduced from the fact that I is proportional to $F^2 L_p$, where I is the intensity of a particular reflection, F is the structural factor, and L_p is the Lorentz polarization. From this, the expression

$$I_{sym}/I_{asym} = F^2_{sym}/F^2_{asym} \quad \text{(Eq. 3)}$$

follows, where I_{sym} and I_{asym} are the intensities of a basal reflection in cases where the two types of octahedral sheets contain equal and unequal numbers of heavy cations, respectively. In chlorites, F_{sym} for the (003) reflection is 106.83, whereas the structural factor F_{asym} for the asymmetrical distribution is (106.83) – (degree of asymmetry)*(13.135). The degree of asymmetry is deduced from the ratio $I(003)/I(005)$, and the value 13.135 is the difference between the effective diffracting powers (atomic scattering factors) of Fe and Mg for the (003) reflection of chlorite irradiated with copper radiation (International Tables of Crystallography, 1974, pp.71–79; 1992, pp. 477–499). It follows that

$$I_{sym} = [I(003)_{asym(observed)}][(106.83)^2]/[106.83 - (\text{degree of asymmetry})(13.138)]^2 \quad \text{(Eq. 4)}.$$

I_{sym} is equal to $I(003)_{c*}$, which is the intensity of the third-order basal reflection corrected for asymmetry.

The advantage of this method lies in its simplicity. It does not require comparison of structure factors converted from intensities with theoretically derived absolute values of structure factors, as in the approach of Schoen (1962).

X-ray intensities can only be used to distinguish between Fe (and equivalent heavy ions) and Mg (and equivalent light ions). If the octahedrally coordinated Al ions are unequally distributed in a pure Mg end-member chlorite, so that the ^{VI}Al:Mg ratio differs in the two sheets, then X-ray intensity measurements will give no indication of this situation, simply because the difference in the scattering power of the two cations is too

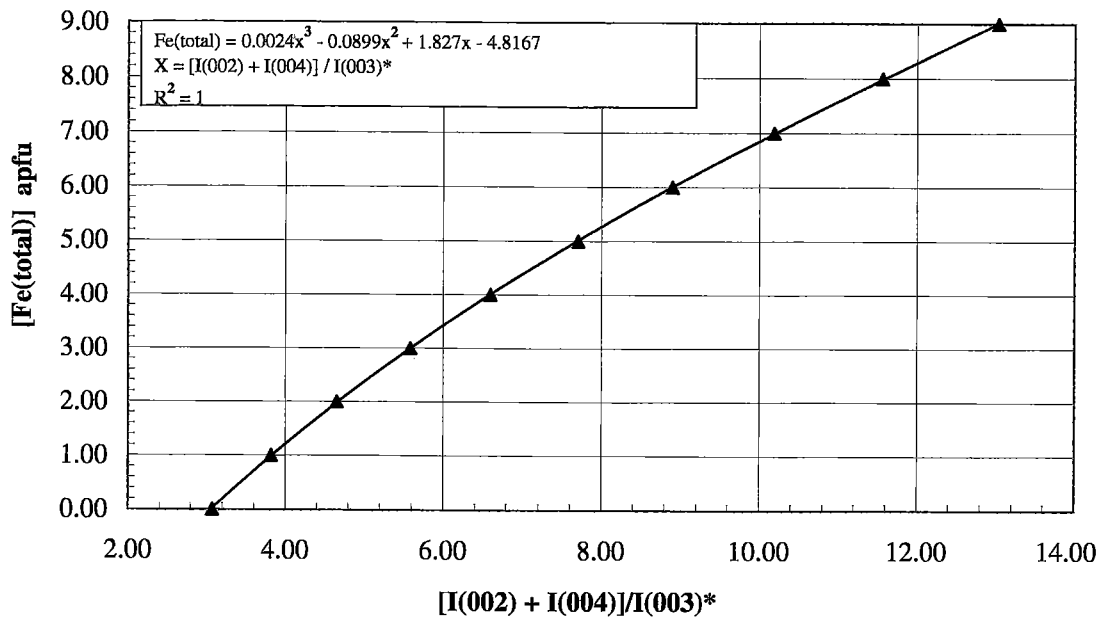

FIG. 4. Determination of total Fe in chlorites using the corrected intensity ratio.

small to be detected. Likewise, X-ray intensities cannot be used to distinguish between Fe^{2+} and Fe^{3+}.

Procedure for Determination of the Complete Formula of a Chlorite

Calculation of structural formula

In the present study, we assume that heavy cations in chlorite are present only in the octahedral sites (*i.e.*, no Fe^{3+} occurs in the tetrahedral sites). All octahedrally coordinated sites of the talc-like layer are available for divalent cations and Fe^{3+}, if necessary. Brucite-like sheets are available for Al^{3+} ions replacing divalent ions (Mg^{2+}, Fe^{2+}) in six-fold coordination, as established earlier by Albee (1962), Shirozu & Bailey (1965), Petruk (1964), Shirozu (1980), and Bailey (1988b). Charge balance is used to calculate the amount of Fe in the Fe^{3+} form.

On the basis of a comparison of compositions determined by electron-microprobe analysis and those calculated from the corrected intensities and spacings of (00*l*) planes, both [^{IV}Al] and total heavy cations in octahedrally coordinated sites were determined with an average precision of 10%.

With the program that was developed to calculate the complete formula of chlorite using the structure factors derived from the relative intensity of particular basal reflections, all the important parameters of chlorite composition can be calculated (for details, see Table 1, 2 and Appendix).

In contrast to Radoslovich's (1962) method and Petruk's (1964) approach, the method developed here gives the complete structural formula for chlorite. In other words, the present method does not only estimate the total proportion of heavy cations in the octahedrally coordinated sites and their distribution between the talc-like layer and brucite-like sheet (*asymmetry*), it also estimates the distribution of [Al] between tetrahedrally and octahedrally coordinated sites. Furthermore, it allows one to calculate the proportion of Fe^{3+} in the octahedral sites of the brucite-like layer (Nelson & Guggenheim 1993).

The precision of the determination of the total Fe by the present program is considerably improved (Table 3) over that attainable with Petruk's (1964) and Radoslovich's (1962) methods. The higher precision is related to the precaution adhered to during sample preparation and XRD analysis as well as the special considerations taken in converting intensities to structure factors and using the calculated concentrations (N) of Si, ^{IV}Al, and ^{VI}Al.

Chlorite in the McGerrigle Mountains Pluton: VLMG Aureole Versus Burial Diagenesis

The study aimed to evaluate the chemical variations of chlorite during progressive diagenesis and metamorphism in an area surrounding the McGerrigle Mountains pluton in the southeastern part of the Taconic belt of Gaspé Peninsula (Fig. 1; Bourque 1989). Another objective was to elucidate the relationship between chlorite composition and the chlorite crystallinity index ChC ($\Delta 2\theta$) as monitored by the full width at half maximum [FWHM] of the $(002)_{14Å}$ reflection in different-size fractions of chlorite.

The chemical composition of chlorite samples calculated using XRD intensities is given in Table 4. The average composition representing the burial-diagenetic samples is

$$(Mg_{2.81}\,Fe^{2+}_{3.16})(Si_{5.44}\,Al_{2.56})O_{20}(OH)_4$$
$$(Fe^{3+}_{0.12}\,Al_{2.66}\,Mg_{1.15}\,Fe^{2+}_{1.99}\,\square_{0.11})(OH)_{12},$$

TABLE 1. PROCEDURE FOR DETERMINATION OF THE COMPLETE FORMULA OF A CHLORITE

Step	Element	Method of Calculation
(1)	The proportion of Fe(total) in octahedrally coordinated sites, in *apfu*	From the $[I(002) + I(004)]/I(003)_{c}$ in program Str-c.xls (Appendix)
(2)	The asymmetry in the distribution of [Fe] between octahedrally coordinated sites of the talc-like layer and of the brucite-like sheet	From I(003)/I(005) in Input-sy.xls (Appendix 1)
(3)	The proportion of Fe^{3+} in octahedral sites of the brucite-like sheet	From the charge-balance postulate: charge on the tetrahedron layer = charge on the octahedron layers
(4)	The proportion of Si^{4+} in tetrahedron sheets	From Eq. 1 using *d*(003)
(5)	The proportion of Al^{3+} in tetrahedrally coordinated sites	From (8 – Si)
(6)	The proportion of Al^{3+} in brucite-like-sheets	From Eq. 2 using *d*(005)
(7)	The overall proportion of Fe^{2+} in octahedrally coordinated sites	From [Fe(total)] – Fe^{3+}
(8)	The proportion of Fe^{2+} in octahedrally coordinated sites of the talc-like layer	From ([Fe(total)] + asymmetry)/2
(9)	The [Fe(total)] (Fe^{2+} + Fe^{3+}) in octahedrally coordinated sites of the brucite-like layer	From [Fe(total)] in octahedrally coordinated sites of the talc-like layer – asymmetry
(10)	The proportion of Fe^{2+} in the brucite-like sheet	From [Fe(total)] in the octahedrally coordinated sites of the brucite-like layer – [Fe^{3+}]
(11)	The proportion of Mg^{2+} in octahedrally coordinated sites	From the total number of cations in the octahedrally coordinated sites, taking into consideration the possibility of vacancies
(12)	The proportion of Mg^{2+} in octahedral coordinated sites of the brucite-like sheet	From compensation of the charge in the tetrahedron sheets
(13)	The proportion of Mg^{2+} in octahedrally coordinated sites of the talc-like layer	From total [Mg] in the octahedrally coordinated sites – [Mg] in the brucite-like sheet

TABLE 2A. DETERMINATION OF Fe-ASYMMETRY BASED ON STRUCTURE-FACTOR RATIO [*F*(003)/*F*(005)]

INPUT DATA

Intensity cps		$I/(Lp\,{}^*\phi)=\|F^2\|$	F(00l)	F(003)/F(005)			
I(001)	84	0.00067	0.02594				
I(002)	4582	0.04549	0.21329				
I(003)	1560	0.13559	0.36823		Ln(X)		
I(004)	4480	0.18250	0.42720	0.92371	-0.0793547	0.83404	
I(005)	864	0.15892	0.39864				
d (003)	4.721						
d (005)	2.831						
d (060)	1.54						
6*d* (060)	9.24						

D=Symmetry 0.835

Si	^{IV}Al	Fe^{3+}
5.262	2.738	0
^{VI}Al + ^{IV}Al	^{VI}Al	
5.596	2.857	

lp=72.35
2θ=18.761
$(Mg_{3.424},Fe^{2+}_{6.00}Fe^{3+}_{0.00}Al_{2.576}(Al_{2.487}Si_{5.513})O_{20}(OH)_{16}$

D= 0
Fe(total)= 6
sinθ/λ=0.1058

Element	N	Z	fa	2πlz	cos2πlz	+F	-F	*F(003)*
Mg	1.57	0.000	9.623	0.000	1.000	15.122		
Al	1.43	0.000	9.707	0.000	1.000	13.866		
Fe^{2+}	3.00	0.000	22.761	0.000	1.000	68.284		
O(OH)	6.00	0.072	7.861	1.358	0.211	9.974		
Si	2.63	0.193	9.765	3.639	-0.879		-22.573	
Al	1.37	0.193	9.707	3.639	-0.879		-11.675	
O	6.00	0.235	7.861	4.431	-0.277		-13.078	
OH	6.00	0.435	7.861	8.203	-0.342		-16.123	
Mg	1.57	0.500	9.623	9.429	-1.000		-15.122	
Al	1.43	0.500	9.707	9.429	-1.000		-13.866	
Fe^{2+}	3.00	0.500	22.761	9.429	-1.000		-68.284	
Fe^{3+}	0.00	0.500	21.971	9.429	-1.000		0.000	
OH	6.00	0.565	7.861	10.654	-0.335		-15.787	
O	6.00	0.765	7.861	14.426	-0.285		-13.422	
Si	2.63	0.807	9.765	15.218	-0.882		-22.666	
Al	1.37	0.807	9.707	15.218	-0.882		-11.723	
O(OH)	6.00	0.928	7.861	17.499	0.219	10.324		
Total						117.570	-224.319	*-106.75*

1/2 octahedral layer
1/2 talc-like layer
tetrahedral layer
octahedral layer
brucite-like sheet
tetrahedral layer
1/2 talc-like layer
1/2 octahedral layer

lp=24.490
2θ=31.418273
$(Mg_{3.424}Fe^{2+}_{6.00}Fe^{3+}_{0.00}Al_{2.576}(Al_{2.487}Si_{5.513})O_{20}(OH)_{16}$

D = 0
Fe(total) = 6
nθ/λ=0.1757

Element	N	Z	*fa*	2πlz	cos2πlz	+F	-F	*F(005)*
Mg	1.57	0.000	9.013	0.000	1.000	14.164		
Al	1.43	0.000	9.223	0.000	1.000	13.175		
Fe^{2+}	3.00	0.000	20.895	0.000	1.000	62.686		
Fe^{3+}	0.00	0.000	20.370	0.000	1.000	0.000		
O(OH)	6.00	0.072	6.132	2.263	-0.638		-23.478	
Si	2.63	0.193	9.372	6.066	0.976	24.078		
Al	1.37	0.193	9.223	6.066	0.976	12.328		
O	6.00	0.235	6.132	7.386	0.451	16.606		
OH	6.00	0.435	6.132	13.671	0.449	16.523		
Mg	1.57	0.500	9.013	15.714	-1.000		-14.164	
Al	1.43	0.500	9.223	15.714	-1.000		-13.175	
Fe^{2+}	3.00	0.500	20.895	15.714	-1.000		-62.686	
Fe^{3+}	0.00	0.500	20.370	15.714	-1.000		0.000	
OH	6.00	0.565	6.132	17.757	0.460	16.937		
O	6.00	0.765	6.132	24.043	0.463	17.020		
Si	2.63	0.807	9.372	25.363	0.974	24.008		
Al	1.37	0.807	9.223	25.363	0.974	12.293		
O(OH)	6.00	0.928	6.132	29.166	-0.628		-23.118	
Total						229.817	-136.621	93.20

1/2 octahedral layer
1/2 talc-like layer
Tetrahedral layer
Octahedral layer
brucite-like sheet
Tetrahedral layer
1/2 talc-like layer
1/2 octahedral layer

The Fa is the value of chemically significant ions...O- The total Fe in the octahedral sites is =6, D = Fe-asymmetry
The calculations taken in cosideration the scattering contribution of actual ^{IV}Al, ^{VI}Al and Si

N = The number of atoms or ions per unit cell; fa = The mean scattering factor value for chemically significant ions;
Z = The fractional coordinate of the atom normal to the (001) reflection. l = An integer denoting of the order of the basal reflection

TABLE 2B. ESTIMATION OF THE TOTAL IRON CONTENT AND STRUCTURAL FORMULA OF CHLORITE

lp=167.482
2θ=12.510

D = 0
Fe(total) = 6
Fe^{3+} = 0

Element	N	Z	fa	2πlz	cos2πlz	+F	-F	*F(002)*
Mg	4.54	0.000	*9.829*	0.000	1.000	44.653		
Al	1.46	0.000	*9.867*	0.000	1.000	14.376		
Fe^{2+}	0.00	0.000	*23.43*	0.000	1.000	0.000		
O(OH)	6.00	0.072	*8.586*	0.905	0.618	31.832		
Si	2.63	0.193	*9.894*	2.425	-0.754		-19.656	
Al	1.37	0.193	*9.867*	2.425	-0.754		-10.166	
O	6.00	0.235	*8.586*	2.953	-0.982		-50.604	
OH	6.00	0.435	*8.586*	5.466	0.649	33.413		
Mg	4.54	0.500	*9.829*	6.283	1.000	44.653		
Al	1.46	0.500	*9.867*	6.283	1.000	14.376		
Fe^{2+}	0.00	0.500	*23.43*	6.283	1.000	0.000		
Fe^{3+}	0.00	0.500	*22.529*	6.283	1.000	0.000		
OH	6.00	0.565	*8.586*	7.100	0.685	35.265		
O	6.00	0.765	*8.586*	9.613	-0.982		-50.604	
Si	2.63	0.807	*9.894*	10.141	-0.754		-19.656	
Al	1.37	0.807	*9.867*	10.141	-0.754		-10.166	
O(OH)	6.00	0.928	*8.586*	11.662	0.618	31.832		
Total						250.401	-160.853	*89.5481*

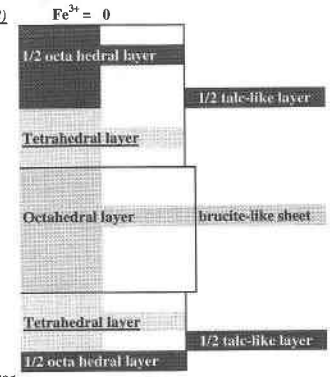

D = 0
Fe(total) = 6
Fe^{3+} = 0

Element	N	Z	fa	2πlz	cos2πlz	+F	-F	*F(004)*
Mg	4.54	0.000	*9.344*	0.000	1.000	42.450		
Al	1.46	0.000	*9.487*	0.000	1.000	13.823		
Fe^{2+}	0.00	0.000	*21.890*	0.000	1.000	0.000		
O(OH)	6.00	0.072	*7.011*	1.810	-0.236	-9.949		
Si	2.63	0.193	*9.588*	4.851	0.138	3.480		
Al	1.37	0.193	*9.487*	4.851	0.138	1.786		
O	6.00	0.235	*7.011*	5.906	0.930	39.112		
OH	6.00	0.435	*7.011*	10.933	-0.063		-2.641	
Mg	4.54	0.500	*9.344*	12.566	1.000	42.450		
Al	1.46	0.500	*9.487*	12.566	1.000	13.823		
Fe^{2+}	0.00	0.500	*21.890*	12.566	1.000	0.000		
Fe^{3+}	0.00	0.500	*21.230*	12.566	1.000	0.000		
OH	6.00	0.565	*7.011*	14.200	-0.063		-2.641	
O	6.00	0.765	*7.011*	19.227	0.930	39.112		
Si	2.63	0.807	*9.588*	20.282	0.138	3.480		
Al	1.37	0.807	*9.487*	20.282	0.138	1.786		
O(OH)	6.00	0.928	7.011	23.323	-0.236		-9.948	
Total						191.351	-15.231	176.12

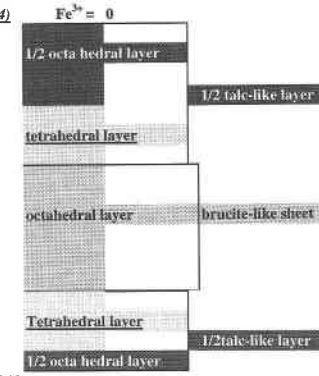

Input data						
I(001)	84					
I(002)	4582		13829.43			
I(003)	1560	I(003)*	1287.27	I(002)+I(004)/I(	7.03970402	4.375208
I(004)	4480				4.37520753	
I(005)	864			Total Fe	4.375	

Total no. of Fe in octahedral sites	4.375
(Symmetry) Fe in talc - Fe in brucite	0.820
Number of Fe^{3+} in the brucite-like layer	0.000
X(Si) from d(005)	5.268
Number of Al atoms in tetrahedral sites	2.732
Number of Al atoms in the octahedral sites of the brucite-like sheet	2.914
Total number of Fe^{2+} atoms in octahedral sites	4.375
Number of Fe^{2+} atoms in octahedral sites in 2:1 layer	2.598
Total number of Fe (Fe^{2+} + Fe^{3+}) atoms in octahedral sites of the brucite-like sheet	1.778
Number of Fe^{2+} atoms in Brucite like sheet	1.778
Number of Mg^{2+} atoms in octahedral sites	4.620
Number of Mg^{2+} atoms in octahedral sites of the brucite sheet	1.218
Number of Mg^{2+} atoms in octahedral sites of the 2:1 layer	3.403
Vacancy in the octahedral sites	0.091

$$(Mg_{3.403}\ Fe^{2+}_{2.598})\ (Al_{2.732}\ Si_{5.268})\ O_{20}\ (OH)_4$$
$$(Fe^{3+}_{0.000}\ Al_{2.914}\ Mg_{1.218}\ Fe^{2+}_{1.778}\ \square_{0.091})\ (OH)_{12}$$

whereas the average composition of chlorite from the anchizone around the McGerrigle Mountain pluton is

$$(Mg_{3.16}Fe^{2+}_{2.75})(Si_{5.26}Al_{2.74})O_{20}(OH)_4$$
$$(Fe^{3+}_{0.11}Al_{2.79}Mg_{1.67}Fe^{2+}_{1.44}\square_{0.08})(OH)_{12}.$$

The [^{IV}Al] values range from 2.56 to 2.93 *apfu* (out of the theoretical 8.0 tetrahedral sites) in the fine fraction (<0.1 μm) of burial diagenetic samples, with an average of 2.70 *apfu*. The range of [^{IV}Al] in the coarse fraction (<2 μm) of the samples is 2.03 to 2.84 *apfu*, with an average of 2.41 *apfu*. On the other hand, in the anchizone samples, the ranges of [^{IV}Al] in the fine and coarse fractions are 2.60–2.98 and 2.45–2.93 *apfu*, with averages of 2.85 and 2.64 *apfu*, respectively. The [^{IV}Al] values increase with improving chlorite crystallinity.

On average, the total octahedrally coordinated cations in the burial-diagenetic samples amount to 11.89 *apfu*, and 11.92 *apfu* in the anchizone. Figure 5 shows the relationship between the [Si] and [R^{2+}] (total octahedrally coordinated divalent cations), together with the corresponding proportion of R^{3+} (total Al and Fe^{3+}), and occupancy of the octahedral sites (Σ^{VI}). In general, metamorphic chlorites from the McGerrigle anchizone tend to plot along or close to the line of full octahedral occupancy between serpentine and amesite, whereas the burial-diagenetic samples show a greater scatter (Fig. 5) on the vector representation of Wiewióra & Weiss (1990). Grain size is weakly correlated with the total occupancy of the octahedral sites, but a stronger correlation exists with [R^{3+}]. The occupancy of the octahedral sites appears to increase in the finer fractions, but the large dispersion in the data does not indicate a clear trend (Fig. 5). However, the total occupancy of the octahedral sites is better correlated with the chlorite (ChC) and illite crystallinity (IC) indices (not shown).

The ratio [Fe]/[(Fe + Mg)] in chlorite formed in burial diagenetic and very low-grade metamorphic pelitic rocks of the McGerrigle Mountains ranges from 0.37 to 0.83 and from 0.36 to 0.71, respectively. In terms of chlorite composition, "pycnochlorite" and "ripidolite" are fairly Fe-rich chlorites (Fig. 6). Furthermore, the [Si] and [Fe]/[(Fe + Mg)] value of the chlorite are a function of diagenetic and metamorphic conditions and, to a lesser extent, of grain size. High-grade diagenetic samples have a relatively large range of [Si] and [Fe]/[(Fe + Mg)] values compared to the samples from the anchizone around McGerrigle Mountains pluton.

Relationships between chlorite composition and maturation indices (chlorite and illite crystallinity indices) are given in Figures 6 and 7. In the burial-diagenetic samples, both [Fe]/[(Fe + Mg)] and [^{IV}Al] increase with improving chlorite crystallinity on the basis of comparison of values in the coarse- and fine-grained fractions of each sample. In the McGerrigle Mountains anchizone, the reverse trend prevails, *i.e.*, the [Fe]/[(Fe + Mg)] ratio decreases with increasing metamorphic grade.

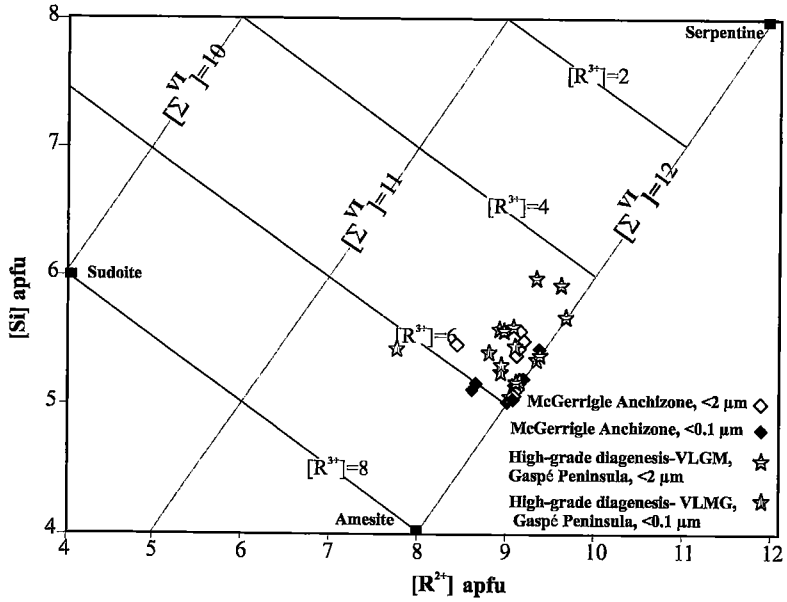

FIG. 5. Chlorite compositions plotted in the vector representation of Wiewióra & Weiss (1990), with [Si] and [R^{2+}] as coordinate axes, and [R^{3+}] octahedral occupancy shown by orthogonal isolines.

TABLE 3. COMPARISON OF ESTIMATED [Fe-TOTAL] BY METHOD OF PETRUK (1964) AND PRESENT STUDY

Sample	Intensity (cps)				*d* spacing (Å)		Chemical composition (EPM data)						Petruk 1964 method				*#Fe-total*
no.	I2	I3	I4	I5	*d* 003	*d* 005	Si	^{IV}Al	^{VI}Al	Mg	Fe	Mn	I3/I5	D	I(003)*	**Fe	
[3]	8968	3034	7872	1600	4.729	2.835	5.55	2.45	2.32	5.51	**4.19**	0.02	1.896	*1.25*	5805	**2.9(-31%)**	***3.972(-5.16%)***
	$(Mg_{5.51}\ Fe^{2+}_{4.10})(Fe^{3+}_{0.09}\ Al_{2.32})(Si_{5.55}\ Al_{2.45})O_{20}\ (OH)_{16}$																
	$(Mg_{3.645}Fe^{2+}_{2.356})(Si_{5.431}Al_{2.569})O_{20}(OH)_4\ (Fe^{3+}_{0.000}Al_{2.604}Mg_{1.762}Fe^{2+}_{1.617}\square_{0.018})(OH)_{12}$																
[4]	4133	2067	4214	1071	4.728	2.833	5.49	2.51	2.88	6.69	**2.21**	0.01	1.93	*1.22*	3883	**2.15(-3.15%)**	***2.08(-5.88%)***
	$(Mg_{6.69}\ Fe^{2+}_{2.14})(Fe^{3+}_{0.07}\ Al_{2.88})(Si_{5.49}\ Al_{2.51})O_{20}\ (OH)_{16}$																
	$(Mg_{4.609}Fe^{2+}_{1.391})(Al_{2.596}Si_{5.404})O_{20}(OH)_4\ (Fe^{3+}_{0.000}Al_{2.819}Mg_{2.385}Fe^{2+}_{0.685}\square_{0.112})(OH)_{12}$																
[5]	6001	1769	5443	1034	4.727	2.834	5.17	2.83	2.76	3.94	**5.28**	0.02	1.71	*1.51*	3996	**2.86(-46%)**	***5.253(0.44%)***
	$(Mg_{3.94}\ Fe^{2+}_{5.17})(Fe^{3+}_{0.11}\ Al_{2.76})(Si_{5.17}\ Al_{2.83})O_{20}\ (OH)_{16}$																
	$(Mg_{2.905}Fe^{2+}_{3.095})(Al_{2.623}Si_{5.377})O_{20}(OH)_4\ (Fe^{3+}_{0.000}Al_{2.641}Mg_{1.192}Fe^{2+}_{2.158}\square_{0.009})(OH)_{12}$																
[6]	4852	1560	4480	864	4.721	2.831	5.36	2.64	2.78	4.64	**4.44**	0.01	1.81	*1.38*	3231	**2.89(-35.1%)**	***4.585(3.24%)***
	$(Mg_{4.64}\ Fe^{2+}_{4.30})(Fe^{3+}_{0.14}\ Al_{2.78})(Si_{5.36}\ Al_{2.64})O_{20}\ (OH)_{16}$																
	$(Mg_{3.291}Fe^{2+}_{2.710})(Al_{2.732}Si_{5.268})O_{20}(OH)_4\ (Fe^{3+}_{0.000}Al_{2.914}Mg_{1.120}Fe^{2+}_{1.875}\square_{0.091})(OH)_{12}$																
[7]	7541	3012	7407	1649	4.739	2.838	5.45	2.55	2.36	6.11	**3.60**	0.01	1.827	*1.37*	6207	**2.41(-33.2%)**	***3.391(-5.81%)***
	$(Mg_{6.11}\ Fe^{2+}_{3.55})(Fe^{3+}_{0.05}\ Al_{2.36})(Si_{5.45}\ Al_{2.55})O_{20}\ (OH)_{16}$																
	$(Mg_{3.900}Fe^{2+}_{2.101})(Al_{2.363}Si_{5.637})O_{20}(OH)_4\ (Fe^{3+}_{0.000}Al_{2.538}Mg_{2.084}Fe^{2+}_{1.291}\square_{0.088})(OH)_{12}$																
[44]	8074	2632	8031	1535	4.744	2.843	5.71	2.29	2.10	5.29	**4.64**	0.04	1.72	*1.44*	5678	**2.84(-39.3%)**	***4.708(1.57%)***
	$(Mg_{5.29}\ Fe^{2+}_{4.51})(Fe^{3+}_{0.13}\ Al_{2.10})(Si_{5.71}\ Al_{2.29})O_{20}\ (OH)_{16}$																
	$(Mg_{3.178}Fe^{2+}_{2.823})(Si_{5.732}Al_{2.268})O_{20}(OH)_4\ (Fe^{3+}_{0.128}Al_{2.140}Mg_{1.975}Fe^{2+}_{1.758}\square_{0.000})(OH)_{12}$																
[45]	9572	2706	9062	1588	4.734	2.839	5.80	2.20	2.24	4.24	**5.48**	0.01	1.70	*1.43*	5799	**3.21(-41.5%)**	***5.572(1.7%)***
	$(Mg_{4.24}\ Fe^{2+}_{5.44})(Fe^{3+}_{0.04}\ Al_{2.24})(Si_{5.80}\ Al_{2.20})O_{20}\ (OH)_{16}$																
	$(Mg_{2.740}Fe^{2+}_{3.155})(Si_{5.536}Al_{2.464})O_{20}(OH)_4\ (Fe^{3+}_{0.000}Al_{2.357}Mg_{1.280}Fe^{2+}_{2.312}\square_{0.051})(OH)_{12}$																
[46]	8589	3160	8825	1813	4.728	2.832	5.42	2.58	2.72	5.08	**4.09**	0.01	1.74	*1.44*	6803	**2.56-(37.4%)**	***4.156(1.59%)***
	$(Mg_{5.08}\ Fe^{2+}_{4.01})(Fe^{3+}_{0.08}\ Al_{2.72})(Si_{5.42}\ Al_{2.58})O_{20}\ (OH)_{16}$																
	$(Mg_{3.472}Fe^{2+}_{2.528})(Si_{5.410}Al_{2.590})O_{20}(OH)_4\ (Fe^{3+}_{0.000}Al_{2925}Mg_{1.280}Fe^{2+}_{1.628}\square_{0.018})(OH)_{12}$																

The [Mg]/[Fe] value of the fine and coarse fractions in the burial diagenetic samples ranges from 0.25 to 1.11 and from 021 to 1.68, with averages of 0.74 and 1.05, respectively. In the McGerrigle Mountains anchizone, the [Mg]/[Fe] value of the fine and coarse fractions ranges from 0.41 to 1.82 and from 0.52 to 2.16, with averages of 1.11 and 1.25, respectively. The scatter in the [Mg]/[Fe] values in the coarse fractions is large. The overall picture reveals a relatively good correlation between [Mg]/[Fe] and ChC, showing an increase in [Mg]/[Fe] as chlorite crystallinity improves (Fig. 8).

The ratio [Mg + Al]/[Fe] shows a trend similar to that of [Mg]/[Fe]. The average values of [(Mg + Al)]/[Fe] in the coarse and fine fractions of burial diagenetic environments are 3.70 and 3.43, respectively, whereas in the anchizone, they are 3.42 and 3.24, respectively. Both [Mg]/[Fe] and ([Mg + Al])/[Fe] are fairly well correlated positively with chlorite crystallinity and grain size, showing an increase with improving ChC.

The inferred distribution of Fe atoms between the two types of octahedral sites of chlorite-group minerals is related to ChC. The Fe-asymmetry increases with decreasing ChC in the coarse fractions (Fig. 9a), this effect being coupled with decreasing [Fe(total)] in the octahedral site. The rate of decrease of [Fe] in the brucite-like sheet seems higher than that in the talc-like layer under metamorphic conditions. In contrast, the [Fe (total)] in the octahedral site increases with decreasing asymmetry and improving chlorite crystallinity in the diagenetic samples (Fig. 9b). This correlation may be interpreted as the result of preferential incorporation of Fe in the brucite-like sheet. The same trend can be observed if Fe-asymmetry is compared with IC as another indicator of maturity. The dispersion of the data on Fe-asymmetry in the <2 μm fraction crystals may be related to the contribution of detrital chlorite. Shata and Hesse (in prep.) show that the coarse fractions (<2 μm) are a product of Ostwald ripening under VLGM condi-

[47]	1665	1528	3450	1006	4.755	2.843	5.55	2.45	2.73	7.43	**1.66**	0.02	1.52	*1.61*	3694	**1.39(-17%)**	*1.62(-2.53%)*
	$(Mg_{7.49}Fe^{2+}_{1.58})(Fe^{3+}_{0.08}Al_{2.73})(Si_{5.55}Al_{2.45})O_{20}(OH)_{16}$																
	$(Mg_{4.609}Fe^{2+}_{1.391})(Si_{5.971}Al_{2.029})O_{20}(OH)_4(Fe^{3+}_{0.000}Al_{2.339}Mg_{3.277}Fe^{2+}_{0.229}\square_{0.155})(OH)_{12}$																
[53]	3464	2089	4853	1207	4.724	2.833	5.68	2.32	2.43	7.03	**2.46**	0.00	1.73	*1.42*	4448	**1.78(-27.6%)**	*2.253(-8.41%)*
	$(Mg_{7.03}Fe^{2+}_{2.41})(Fe^{3+}_{0.05}Al_{2.43})(Si_{5.68}Al_{2.32})O_{20}(OH)_{16}$																
	$(Mg_{4.416}Fe^{2+}_{1.584})(Si_{5.328}Al_{2.672})O_{20}(OH)_4(Fe^{3+}_{0.000}Al_{2.682}Mg_{2.644}Fe^{2+}_{0.669}\square_{0.005})(OH)_{12}$																
[54]	11422	4947	11860	2686	4.733	2.836	5.48	2.52	2.76	6.12	**3.00**	0.00	1.84	*1.31*	9823	**2.37(-21%)**	*3.051(1.7%)*
	$(Mg_{6.12}Fe^{2+}_{3.00})(Fe^{3+}_{0.00}Al_{2.76})(Si_{5.48}Al_{2.52})O_{20}(OH)_{16}$																
	$(Mg_{4.077}Fe^{2+}_{1.923})(Si_{5.513}Al_{2.487})O_{20}(OH)_4(Fe^{3+}_{0.000}Al_{2.576}Mg_{2.252}Fe^{2+}_{1.128}\square_{0.045})(OH)_{12}$																
[66]	1341	324	835	201	4.736	2.837	5.63	2.37	2.22	4.31	**5.41**	0.01	1.61	*1.65*	3129	**2.34(-56.8%)**	*5.681(5.03%)*
	$(Mg_{4.31}Fe^{2+}_{5.14})(Fe^{3+}_{0.27}Al_{2.22})(Si_{5.63}Al_{2.37})O_{20}(OH)_{16}$																
	$(Mg_{2.635}Fe^{2+}_{0.366})(Si_{5.573}Al_{2.427})O_{20}(OH)_4(Fe^{3+}_{0.000}Al_{2.575}Mg_{1.036}Fe^{2+}_{2.316}\square_{0.074})(OH)_{12}$																
[67]	3428	1030	3144	681	4.725	2.834	5.18	2.82	2.60	4.28	**5.18**	0.04	1.51	*1.69*	2631	**2.5(-52.1%)**	*5.43(4.94%)*
	$(Mg_{4.28}Fe^{2+}_{5.08})(Fe^{3+}_{0.10}Al_{2.60})(Si_{5.18}Al_{2.82})O_{20}(OH)_{16}$																
	$(Mg_{2.697}Fe^{2+}_{3.303})(Si_{5.338}Al_{2.662})O_{20}(OH)_4(Fe^{3+}_{0.060}Al_{2.602}Mg_{1.271}Fe^{2+}_{2.067}\square_{0.000})(OH)_{12}$																
[68]	2717	726	2357	483	4.724	2.832	5.43	2.57	2.57	3.70	**5.66**	0.00	1.503	*1.70*	1873	**2.71(-52.1%)**	*6.171(9.03%)*
	$(Mg_{3.70}Fe^{2+}_{5.52})(Fe^{3+}_{0.14}Al_{2.57})(Si_{5.43}Al_{2.57})O_{20}(OH)_{16}$																
	$(Mg_{2.322}Fe^{2+}_{3.678})(Si_{5.330}Al_{2.670})O_{20}(OH)_4(Fe^{3+}_{0.000}Al_{2.845}Mg_{0.575}Fe^{2+}_{2.493}\square_{0.087})(OH)_{12}$																
[70]	6747	1769	5726	994	4.716	2.830	5.26	2.71	2.74	3.27	**5.87**	0.05	1.78	*1.41*	3743	**3.33(-43.8%)**	*5.73(-2.39%)*
	$(Mg_{3.27}Fe^{2+}_{5.54})(Fe^{3+}_{0.33}Al_{2.71})(Si_{5.26}Al_{2.74})O_{20}(OH)_{16}$																
	$(Mg_{2.704}Fe^{2+}_{3.296})(Si_{5.165}Al_{2.835})O_{20}(OH)_4(Fe^{3+}_{0.000}Al_{2.871}Mg_{0.677}Fe^{2+}_{2.434}\square_{0.018})(OH)_{12}$																
15	2687	1432	3119	839	4.734	2.837	5.52	2.48	2.88	6.64	**2.24**	0.01	1.71	*1.43*	3069	**1.89(-16%)**	*2.385(6.47%)*
	$(Mg_{6.64}Fe^{2+}_{2.19})(Fe^{3+}_{0.06}Al_{2.88})(Si_{5.52}Al_{2.48})O_{20}(OH)_{16}$																
	$(Mg_{4.338}Fe^{2+}_{1.663})(Si_{5.532}Al_{2.468})O_{20}(OH)_4(Fe^{3+}_{0.000}Al_{2.524}Mg_{2.726}Fe^{2+}_{0.723}\square_{0.028})(OH)_{12}$																
62	980	436	1427	320	4.722	2.836	5.85	2.15	2.15	5.16	**4.68**	0.01	1.363	*1.98*	1384	**1.74(-62.9%)**	*4.487(-4.1%)*
	$(Mg_{5.16}Fe^{2+}_{4.66})(Fe^{3+}_{0.02}Al_{2.15})(Si_{5.85}Al_{2.15})O_{20}(OH)_{16}$																
	$(Mg_{3.062}Fe^{2+}_{2.938})(Si_{5.286}Al_{2.714})O_{20}(OH)_4(Fe^{3+}_{0.295}Al_{2.419}Mg_{2.032}Fe^{2+}_{1.254}\square_{0.000})(OH)_{12}$																

Italicized chemical formula shown inside a frame is calculated from electron-microprobe (EPM) data. The formula shown below the frame is established using XRD data and the approach described in this study. **Fe: amount of Fe-total estimated using Petruk's (1964) method. D: Asymmetry. □: vacancy. #Fe-total is the total iron occupying octahedrally coordinated sites, estimated according to the present study. Precision (values shown between parentheses) = [Fe estimated using the present method – Fe (EPM data)]/Fe (EPM data).

tions, whereas the fine fractions (<0.1 μm) are predominantly of diagenetic origin.

Structurally, both Ib and IIb chlorite polytypes exist in the high-grade diagenetic samples. Neither swelling chlorite nor berthierine was observed. Apparently, the IIb polytype is concentrated in the coarse fraction, whereas a mixture of Ib and IIb or only Ib is the main constituent in the fine fraction. On the diagram of Curtis *et al.* (1985), samples with a relatively high [Fe]/[(Fe + Mg)] value are rich in the Ib polytype, whereas those with a low [Fe]/[(Fe + Mg)] value are mainly IIb (Fig. 10). On the other hand, among the anchizonal samples in the suite, the Ib polytype does not occur alone; these samples consist either entirely of IIb polytypes or of a mixture of Ib and IIb, with IIb being dominant.

For trioctahedral layer silicates, the optimum range of [^{IV}Al] should be about 1.0–1.8 *apfu* out of the four available positions (Albee 1962). Cathelineau & Nieva (1985), Bevins *et al.* (1991), and Velde & Medhioub (1988) concluded that [^{IV}Al] in chlorite increases systematically with an increase in temperature. The [^{IV}Al] in metamorphic chlorite in the present study ranges from 2.03 to 2.98 *apfu*. In burial-diagenetic samples, the [^{IV}Al] increases in the finer fractions with improving IC and ChC. Although the range and average of [^{IV}Al] in the anchizone are higher than those in burial diagenetic samples, they are not correlated with grain size. On the other hand, [^{IV}Al] is correlated with IC and ChC.

TABLE 4A. THE STRUCTURAL FORMULA OF CHLORITE (<2 μm) CALCULATED FROM XRD PATTERNS

	A306	A309	A312	A318	A412	ML57	R252	R253	TM6	TM29	TM30	TM39	89-42	H-43	H-44
	Burial diagenetic samples								McGerrigle anchizone samples						
I(002) cps	1651	409	578	360	294	669	1025	1019	359	309	825	112	1354	3214	2961
I(003)	627	181	153	179	73	244	496	458	171	143	332	52	427	1025	638
I(004)	1831	526	799	673	299	599	1689	1630	358	317	803	95	1511	3321	1723
I(005)	312	116	67	125	65	140	248	274	150	100	217	64	300	667	282
d(003) Å	4.7554	4.7405	4.734	4.753	4.726	4.716	4.735	4.734	4.727	4.716	4.729	4.713	4.735	4.7322	4.7285
d(005)	2.843	2.843	2.833	2.844	2.836	2.830	2.834	2.835	2.833	2.830	2.829	2.832	2.835	2.835	2.833
Total no. of Fe in octahedral sites	3.821	3.715	6.697	4.984	7.917	3.78	3.731	4.565	3.533	3.248	3.768	3.669	6.035	5.459	5.284
(Symmetry) Fe in talc - Fe in brucite	0.626	1.126	0.383	1.275	1.753	0.902	0.637	0.981	1.715	1.282	1.152	2.381	1.289	1.142	0.401
Number of Fe^{3+} in the brucite-like sheet	0.000	0.273	0.000	0.000	0.190	0.000	0.000	0.000	0.000	0.000	0.000	0.319	0.000	0.000	0.000
X(Si) from *d*(005)	5.972	5.664	5.535	5.924	5.369	5.161	5.545	5.53	5.386	5.159	5.437	5.103	5.551	5.494	5.416
Number of Al atoms in tetrahedral sites	2.028	2.336	2.465	2.076	2.631	2.839	2.455	2.47	2.614	2.841	2.563	2.897	2.449	2.506	2.584
Number of Al atoms in the brucite-like sheet	2.369	2.063	2.933	2.261	2.441	2.897	2.855	2.751	2.782	2.895	3.195	2.578	2.7	2.698	2.761
Total number of Fe^{2+} atoms in the octahedral sites	3.821	3.442	6.697	4.984	7.727	3.78	3.731	4.565	3.533	3.248	3.768	3.35	6.035	5.459	5.284
Number of Fe^{2+} atoms in octahedral sites of the 2:1 layer	2.2235	2.4205	3.54	3.13	4.835	2.341	2.184	2.773	2.624	2.265	2.46	3.025	3.662	3.3005	2.8425
Number of (Fe^{2+} + Fe^{3+}) atoms in the brucite-like sheet	1.5975	1.2945	3.157	1.855	3.082	1.439	1.547	1.792	0.909	0.983	1.308	0.644	2.373	2.1585	2.4415
Number of Fe^{2+} atoms in the brUcite-like sheet	1.5975	1.0215	3.157	1.855	2.892	1.439	1.547	1.792	0.909	0.983	1.308	0.325	2.373	2.1585	2.4415
Total number of Mg^{2+} atoms in the octahedral sites	5.640	6.222	2.136	4.663	1.642	5.294	5.214	4.544	5.601	5.830	4.721	5.753	3.140	3.747	3.867
Number of Mg^{2+} atoms in the brucite-like sheet	1.863	2.643	0.000	1.792	0.477	1.635	1.398	1.317	2.225	2.095	1.181	2.778	0.801	1.048	0.709
Number of Mg^{2+} atoms in the 2:1 layer	3.7765	3.5795	2.46	2.871	1.165	3.659	3.816	3.227	3.376	3.735	3.54	2.975	2.338	2.6995	3.1575
Vacancy	0.171	0.000	0.234	0.092	0.000	0.025	0.200	0.140	0.084	0.027	0.316	0.000	0.126	0.096	0.089
Total octahedral site cation occupancy	11.830	12.000	11.766	11.908	12.000	11.971	11.800	11.860	11.916	11.973	11.684	12.000	11.875	11.904	11.912
Total Al	4.397	4.399	5.398	4.337	5.072	5.736	5.310	5.221	5.396	5.736	5.758	5.475	5.149	5.204	5.345
R^{2+}	9.461	9.664	8.833	9.647	9.369	9.074	8.945	9.109	9.134	9.078	8.489	9.103	9.175	9.206	9.151
Mg/Fe	1.476	1.675	0.319	0.935	0.207	1.401	1.397	0.995	1.585	1.795	1.253	1.568	0.520	0.686	0.732
(Mg + Al)/Fe	2.096	2.230	0.757	1.389	0.516	2.167	2.163	1.598	2.373	2.686	2.101	2.271	0.968	1.181	1.254
Fe/(Fe + Mg)	0.404	0.374	0.758	0.517	0.828	0.417	0.417	0.501	0.387	0.358	0.444	0.389	0.658	0.593	0.577
$Fe^{2+}/(Fe^{2+}+Mg)$	0.404	0.356	0.758	0.517	0.825	0.417	0.417	0.501	0.387	0.358	0.444	0.368	0.658	0.593	0.577
(Fe + Mg)/Al	3.993	4.817	3.012	4.266	3.916	3.132	3.133	3.311	3.283	3.136	2.657	3.655	3.398	3.412	3.314
Fe(total)/(Mg + Fe)	0.404	0.384	0.758	0.517	0.845	0.417	0.417	0.501	0.387	0.358	0.444	0.403	0.658	0.593	0.577
Chlorite crystallinity (ChC)	0.342	0.451	0.372	0.365	0.318	0.296	0.314	0.335	0.246	0.268	0.2	0.169	0.264	0.3	0.295
Illite crystallinity (IC)	0.364	0.497	0.514	0.379	0.3	0.415	0.51	0.511	0.301	0.787	0.294	0.606	0.403	0.453	0.413

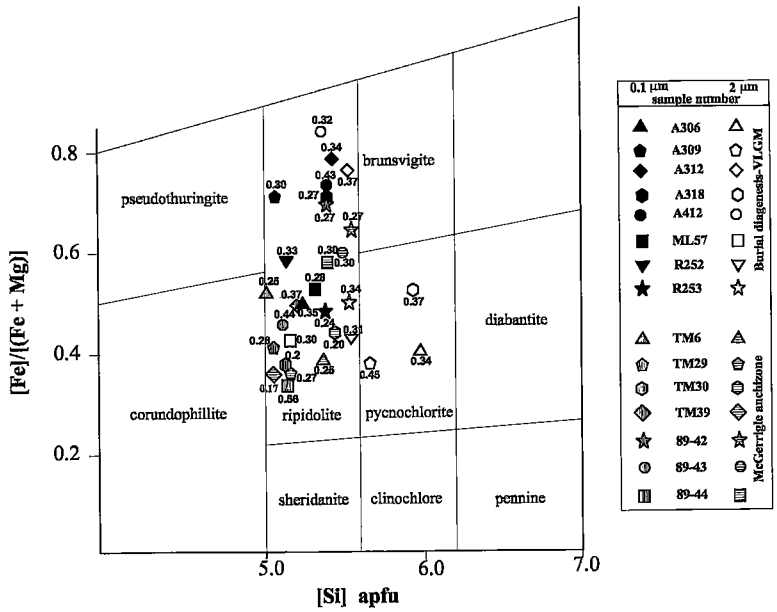

FIG. 6. [Fe]/[(Fe + Mg)] value *versus* [Si], based on 28 atoms of oxygen, for chlorites of different grain-size, different grade, and relationship with chlorite crystallinity.

TABLE 4B. THE STRUCTURAL FORMULA OF CHLORITE (<0.1μm) CALCULATED FROM XRD PATTERNS

	A306	A309	A312	A318	A412	ML57	R252	R253	TM6	TM29	TM30	TM39	H-42	H-43	89-44
	Burial diagenetic samples								McGerrigle anchizone samples						
I(002) cps	1772	396	788	500	279	403	376	954	318	190	282	133	8638	308	113
I(003)	626	111	228	165	68	143	127	333	130	98	128	62	2256	139	48
I(004)	1851	581	1025	605	224	467	543	1036	376	257	310	159	8279	360	114
I(005)	357	74	112	128	77	78	78	166	95	74	79	67	1470	131	26
d(003) Å	4.721	4.712	4.730	4.728	4.728	4.724	4.715	4.727	4.709	4.712	4.714	4.718	4.728	4.714	4.716
d(005)	2.830	2.834	2.824	2.831	2.841	2.831	2.834	2.832	2.827	2.831	2.826	2.832	2.834	2.833	2.827
Total no. of Fe in octahedral sites	4.451	6.954	6.166	6.312	7.326	4.653	5.577	4.287	4.605	3.366	3.269	4.621	6.615	4.201	3.07
(Symmetry) Fe in talc - Fe in brucite	0.89	1.223	0.604	1.48	2.235	0.805	1.055	0.632	1.367	1.444	1.043	2.122	1.145	1.871	0.792
Number of Fe^{3+} in the brucite-like sheet	0.000	0.618	0.000	0.000	0.631	0.000	0.429	0.000	0.000	0.292	0.000	0.140	0.000	0.329	0.000
X(Si) from *d*(005)	5.257	5.067	5.437	5.401	5.401	5.318	5.139	5.385	5.016	5.067	5.108	5.206	5.401	5.113	5.149
Number of Al atoms in tetrahedral sites	2.743	2.933	2.563	2.599	2.599	2.682	2.861	2.615	2.984	2.933	2.892	2.794	2.599	2.887	2.851
Number of Al atoms in the brucite-like sheet	2.98	2.315	3.703	3.01	1.968	2.954	2.432	2.845	2.985	2.641	3.209	2.655	2.665	2.558	3.188
Total number of Fe^{2+} atoms in the octahedral sites	4.451	6.336	6.166	6.312	6.695	4.653	5.148	4.287	4.605	3.074	3.269	4.481	6.615	3.872	3.07
Number of Fe^{2+} atoms in octahedral sites of 2:1 layer	2.6705	4.0885	3.385	3.896	4.781	2.729	3.316	2.46	2.986	2.405	2.156	3.3715	3.88	3.036	1.931
Number of (Fe^{2+}&Fe^{3+}) atoms in the brucite-like sheet	1.7805	2.8655	2.781	2.416	2.546	1.924	2.261	1.828	1.619	0.961	1.113	1.2495	2.735	1.165	1.139
Number of Fe^{2+} atoms in the brucite-like sheet	1.7805	2.2475	2.781	2.416	1.915	1.924	1.832	1.828	1.619	0.669	1.113	1.1095	2.735	0.836	1.139
Total number of Mg^{2+} atoms in the octahedral sites	4.451	2.731	1.561	2.473	2.706	4.257	3.991	4.753	4.410	5.993	5.364	4.723	2.687	5.241	5.574
Number of Mg^{2+} atoms in the brucite-like sheet	1.121	0.820	0.000	0.369	1.487	0.986	1.307	1.213	1.396	2.398	1.520	2.095	0.567	2.277	1.505
Number of Mg^{2+} atoms in the 2:1 layer	3.3295	1.9115	2.615	2.104	1.22	3.271	2.684	3.541	3.014	3.595	3.844	2.6285	2.12	2.964	4.069
Vacancy	0.118	0.000	0.570	0.206	0.000	0.136	0.000	0.115	0.000	0.000	0.159	0.000	0.033	0.000	0.169
Total octahedral site cation occupancy	11.882	12.000	11.430	11.795	12.000	11.864	12.000	11.885	12.000	12.000	11.842	12.000	11.967	12.000	11.832
Total Al	5.723	5.248	6.267	5.609	4.567	5.636	5.293	5.460	5.969	5.574	6.101	5.449	5.264	5.445	6.039
R^{2+}	8.902	9.067	7.726	8.785	9.401	8.910	9.139	9.040	8.995	9.067	8.633	9.205	9.302	9.113	8.644
Mg/Fe	1.000	0.393	0.275	0.392	0.369	0.915	0.716	1.109	0.926	1.431	1.641	1.022	0.406	1.248	1.815
(Mg + Al)/Fe	1.669	0.726	0.886	0.869	0.638	1.550	1.152	1.772	1.567	2.117	2.622	1.597	0.809	1.856	2.854
Fe/(Fe + Mg)	0.500	0.718	0.784	0.719	0.730	0.522	0.583	0.474	0.519	0.411	0.379	0.495	0.711	0.445	0.355
$Fe^{2+}/(Fe^{2+} + Mg)$	0.500	0.699	0.784	0.719	0.712	0.522	0.563	0.474	0.519	0.392	0.379	0.487	0.711	0.425	0.355
(Fe + Mg) /Al	2.987	4.184	2.086	2.918	5.098	3.016	3.934	3.178	3.003	3.544	2.690	3.520	3.490	3.691	2.711
Fe(total)/(Mg + Fe)	0.500	0.767	0.784	0.719	0.779	0.522	0.610	0.474	0.519	0.425	0.379	0.502	0.711	0.461	0.355
Chlorite crystallinity (ChC)	*0.346*	*0.302*	*0.340*	*0.270*	*0.434*	0.281	0.330	0.243	0.249	0.256	0.204	0.366	0.273	0.442	0.559
Illite crystallinity (IC)	*0.324*	*0.335*	*0.489*	*0.440*	*0.661*	0.328	0.307	0.290	0.239	0.565	0.489	0.351	0.416	0.677	0.298

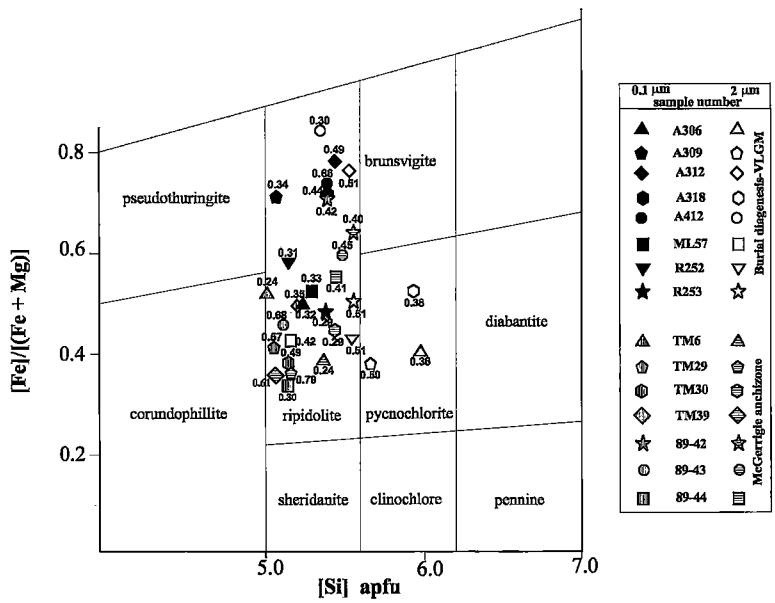

FIG. 7. [Fe]/[(Fe + Mg)] value *versus* [Si], based on 28 atoms of oxygen, for chlorites of different grain-size, different grade, and relationship with illite crystallinity.

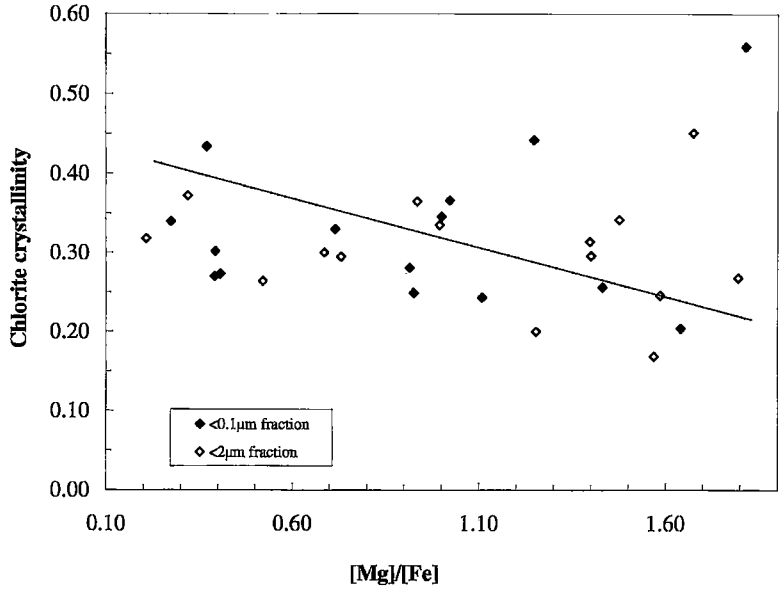

FIG. 8. Effect of [Mg]/[Fe] value and grain-size on chlorite crystallinity (ChC), expressed in °2θ.

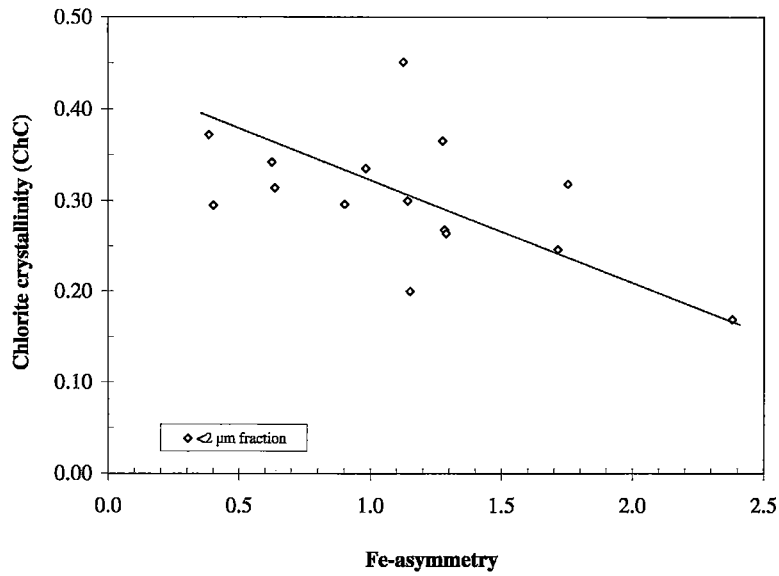

FIG. 9a. The relationship between chlorite crystallinity, expressed in °2θ, and Fe-asymmetry in the <2 μm fraction.

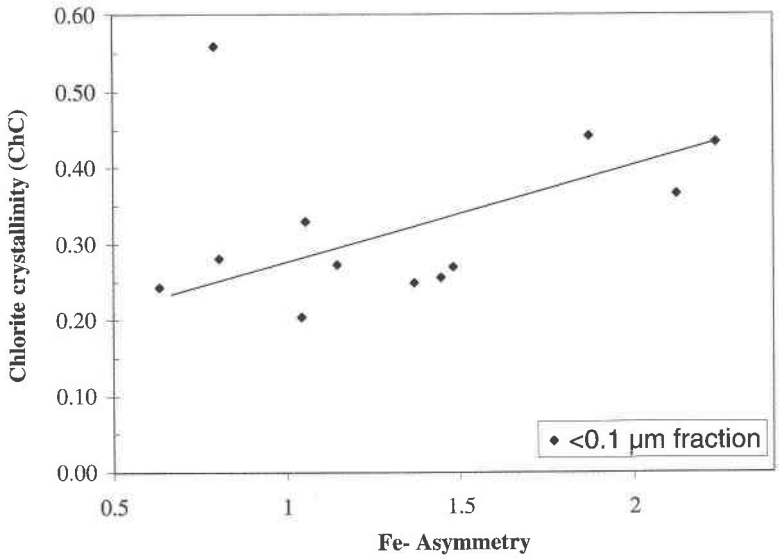

FIG. 9b. The relationship between chlorite crystallinity and Fe-asymmetry in the <0.1μm fraction.

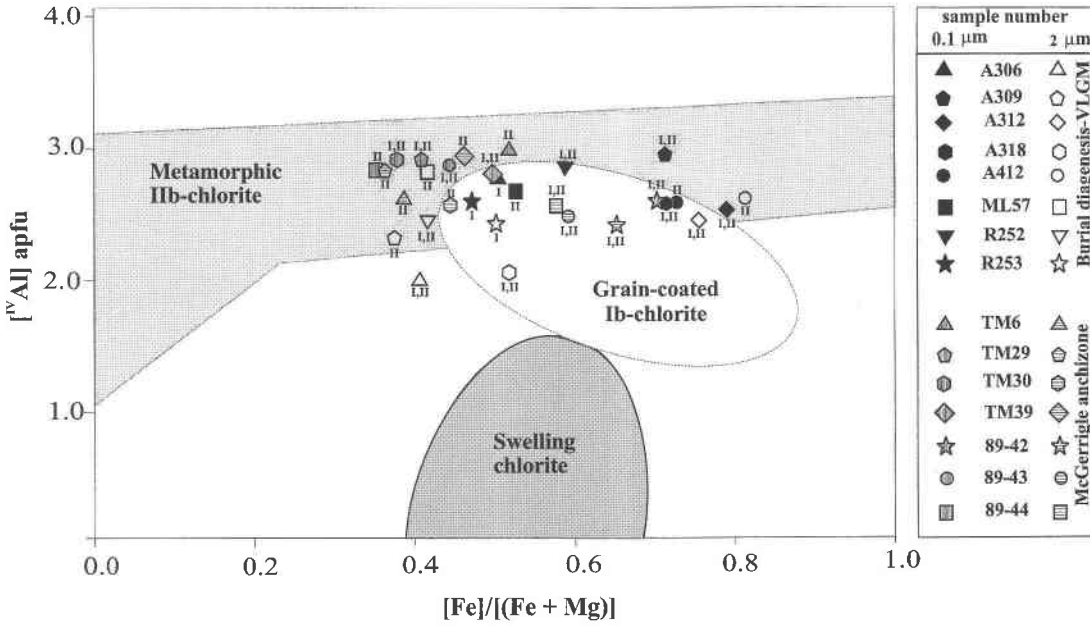

FIG. 10. The relationship among [IV]Al], [Fe]/[(Fe + Mg)] and chlorite polytypes (modified after Curtis *et al.* 1985).

Discussion

The routine XRD method that has been developed in this study to obtain the complete chemical formula of chlorites can be used to replace time-consuming, expensive and complicated analyses by electron microprobe (EMP), scanning electron microscopy (SEM), backscattered electron microscopy (BSE), analytical electron microscopy (AEM), and wet-chemical methods without loss of precision. In the following, the precision of the new method, the chemical changes in chlorite during high-grade diagenesis and very low-grade metamorphism (VLGM) in Gaspé Peninsula, and finally a broad range of applications are discussed.

Precision of the method

The precision of the determination of [Fe(total)] by the present program exceeds that of Petruk (1964) owing to (i) the precautions adhered to during sample preparation and XRD analysis, (ii) accurate calculation of the structure factors, and use of the calculated [Si], [^{IV}Al], and [^{VI}Al]. Moreover, the program gives the complete chemical formula of a trioctahedral chlorite. The spacing of the third and fifth basal reflections is used to calculate the [Si] and [Al], and the charge-balance postulate constrains the [Mg] in the octahedral sites and also the distribution of Mg between the octahedral sheet in the talc-like layer and in the brucite-like sheet. The calculation of [Fe^{3+}] depends on the charge balance between the tetrahedral and octahedral charges, in other words, the difference between the [^{IV}Al] and [^{VI}Al].

Chemical changes of high-grade diagenetic and very low-grade metamorphic terranes of the Gaspé Peninsula

The variable chemical composition of chlorite contains information about the physicochemical conditions of mineral formation. [Fe]/[(Fe + Mg)] is important in the study of phase relationships of low and middle-grade metamorphic rocks (Albee 1962). According to Weaver *et al.* (1984), the [Fe]/[(Fe + Mg)] value of chlorite of very low-grade metamorphic pelitic rocks typically ranges from 0.5 to 0.6, which would indicate a "diabantitic" and "brunsvigitic" composition in Foster's (1962) classification. This generalization compares with ranges from 0.41 to 0.9 and from 0.04 to 0.72 for burial-diagenetic samples and for the anchizone samples, determined in this study, respectively. In both regions, chlorite compositions fall in the field of fairly Fe-rich chlorites, namely "pycnochlorite" and "ripidolite". Brown (1967), Black (1975), and Weaver (1989) noted that [Fe]/[(Fe + Mg)] decreases slightly with the increase of metamorphic grade. However, in rocks of different composition, the ratio is controlled by the bulk-rock composition (Velde & Medhioub 1988, Hillier & Velde 1991). Ruiz Cruz (1997) demonstrated an opposite trend, where a simultaneous increase in [^{IV}Al] and [Fe]/[(Fe + Mg)] occurs with progressive Alpine metamorphism. In the present study, [Fe]/[(Fe + Mg)] decreases with prevailing VLGM conditions. To a lesser extent, [Fe]/[(Fe + Mg)] is related to grain size and maturation index. This correlation can be established only for different grain-size fractions of individual samples, but not for a suite of different samples.

Decreasing [Fe(total)] in the octahedral sites is coupled with increasing Fe-asymmetry in the metamorphic chlorites. This finding may indicate that, in the transition from progressive high-grade diagenesis to VLGM, [Fe] decreases preferentially in the brucite-like sheet. With advancing diagenetic conditions, [Fe(total)] increases, and is coupled with decreasing Fe-asymmetry, which may be interpreted as [Fe] being preferentially incorporated in the brucite-like sheet. Furthermore, strong correlations among [Fe]/[(Mg + Al)], [Mg]/[Fe], [Fe]/[(Fe + Mg)], and chlorite and illite crystallinity have been established by examining the chemical parameters of chlorite in different size-fractions. This is a clear indication that variations in the chlorite chemistry are primarily dependent on bulk-rock chemistry and not on temperature.

According to Árkai (1991), no correlation exists between chlorite crystallinity and the change in chlorite composition, as estimated from the intensity ratios of the basal reflections. In addition, Árkai & Lelkes-Felvári (1993) found that there is no significant correlation among the bulk chemical composition of the main phase, IC and ChC, and that the change in grain size has no significant effect on the crystallinity index of the Hungarian samples of Paleozoic variegated shale that they studied. Dunoyer de Segonzac (1970) stated earlier that the relationship between chemical composition of chlorite and the grade of metamorphism cannot be established with certainty. On the other hand, De Caritat *et al.* (1993) found a decrease in [Si], and an increase in [^{IV}Al], [(Fe + Mg)] and octahedral occupancy with increasing depth of burial, metamorphic grade, or hydrothermal alteration. In the present study, [^{IV}Al] is correlated fairly well with crystallinity index, which is interpreted as being temperature-controlled.

However, for a given mineral association, the increase of [Mg]/[Fe], [(Mg + Al)]/[Fe], octahedral occupancy, as well as the total [Al] content with increasing temperature (as deduced from ChC and IC) may be a valid geothermometer for a restricted range of whole-rock bulk compositions within a given terrane. Furthermore, the change of chlorite composition is not only correlated with the ChC, but also with the change in grain size and polytype. Finally, homogenization in chlorite composition may reflect the VLGM conditions in the aureole of the McGerrigle Mountains pluton.

Applications of the method

The method may be used for the estimation of relative temperature of formation, either based on structural relationships (polytype conversions; De Caritat *et al.*

1993, Walker 1993) or compositional considerations (in a restricted range of whole-rock compositions). According to Cathelineau & Nieva (1985), the proportions of ^{IV}Al and of "octahedral" vacancies are functions of temperature. However, such an inference requires constant bulk-rock composition because, as stated earlier, [Fe]/[(Mg + Fe)] seems to be strongly dependent on composition of the host rock. A decrease in [Si], [^{VI}Al]) and an increase in [^{IV}Al], [Fe + Mg], and the octahedral occupancy [Σ^{VI}] are the main trends with increasing depth of burial, metamorphic grade, or hydrothermal alteration. In other words, the chemical composition of a chlorite, and especially the ratios [Si]/[Al] and [Fe]/[(Fe + Mg)], are a function of the physicochemical conditions of crystallization and the chemical environment of the host rock (Cathelineau & Nieva 1985, Cathelineau 1988, Laird 1988).

The method advocated here is useful for tracing the changes in chemical composition of chlorite from diagenesis to metamorphism, because it allows rapid analyses of large numbers of samples. Chlorites become less siliceous (^{IV}Al increases at the expense of ^{VI}Al), enriched in (Fe + Mg), and octahedral occupancy increases (Hillier & Velde 1991) with advancing VLGM conditions. The method also enables an evaluation of high-temperature diagenesis and hydrothermal alteration, which may have economic implications. Authigenic chlorite provides a record of the diagenetic history, pore-water chemistry and sandstone cementation, where chlorite grain-coatings inhibit quartz cementation and thus may slow down deterioration of a reservoir (Spötl *et al.* 1994, Hesse & Abid 1998).

The method can also be applied to an evaluation of the changes in chlorite composition in the conversion of smectite to chlorite during diagenesis. The [Fe]/[(Fe + Mg)] and ^{IV}Al/Si values increase in the order from smectite to corrensite and chlorite (Shau *et al.* 1990, Schiffman & Fridleifsson 1991, Shau & Peacor 1992).

Conclusions

A new program has been developed to determine the structural formula of chlorite by calculating the total heavy metal content (Y) and the asymmetry (D) of its distribution between the two types of octahedral sites. It calculates the [Fe(total)] with ±10% precision, improving previous XRD-based methods; it also determines the asymmetry in Al distribution and octahedral vacancies, and detects the presence of Fe^{3+}.

The method is applied to the high-grade diagenetic – very low-grade metamorphic chlorites from the Gaspé Peninsula (Quebec Appalachians). During the passage from diagenesis to metamorphism, chlorites become less siliceous, and show increased octahedral-site occupancy (close to ideal trioctahedral chlorite), increased [(Fe + Mg)], [Mg]/[Fe] and [(Mg + Al)]/[Fe], and decreased [Fe]/[(Fe + Mg)]. These parameters seem to depend more on host-rock composition than on temperature of formation.

Decreasing [Fe(total)] in the octahedral site is coupled with increasing asymmetry in the distribution of Fe in metamorphic chlorite, possibly owing to preferential decrease in [Fe(total)] in the brucite-like sheet. In contrast, during early diagenesis, Fe-asymmetry decreases (especially <0.1 μm fraction), whereas the [Fe(total)] increases, possibly owing to the preferential incorporation of Fe in the brucite-like sheet.

Acknowledgements

We are grateful to Prof. MacLean of McGill University for providing all the reference samples, and fruitful discussions. Special thanks are due to M.D. Ruiz Cruz and F. Nieto for their constructive comments, which helped to improve the paper. Critical comments by the editor and an anonymous reviewer are greatly acknowledged. This work was supported by NSERC operating grants to the second author.

References

Ahn, Jung-Ho & Peacor, D.R. (1985): Transmission electron microscopic study of diagenetic chlorite in Gulf Coast argillaceous sediments. *Clays Clay Minerals* **33**, 228-236.

Albee, A.L. (1962): Relationships between the mineral association, chemical composition and physical properties of the chlorite series. *Am. Mineral.* **47**, 851-870.

Árkai, P. (1991): Chlorite crystallinity: an empirical approach and correlation with illite crystallinity, coal rank and mineral facies as exemplified by Palaeozoic and Mesozoic rocks of northeast Hungary. *J. Metamorphic Geol.* **9**, 723-734.

_____ & Lelkes-Felvári, G. (1993): The effects of lithology, bulk chemistry and modal composition on illite "crystallinity" – a case study from the Bakony Mts., Hungary. *Clay Mineral.* **28**, 417-433.

Bailey, S.W. (1972): Determination of chlorite compositions by X-ray spacings and intensities. *Clays Clay Minerals* **20**, 381-388.

_____ (1975): Chlorites. *In* Soil Components. 2. Inorganic Components (J.E. Gieseking, ed.). Springer-Verlag, New York, N.Y. (191-263).

_____ (1988a): X-ray diffraction identification of the polytypes of mica, serpentinite, and chlorite. *Clays Clay Minerals* **36**, 193-213.

_____ (1988b): Chlorites: structures and crystal chemistry. *In* Hydrous Phyllosilicates (Exclusive of Micas) (S.W. Bailey, ed.). *Rev. Mineral.* **19**, 347-403.

Bannister, F.A. & Whittard, W.F. (1945): A magnesian chamosite from the Wenlock limestone of Wickwar, Gloucestershire. *Mineral. Mag.* **27**, 99-111.

BEVINS, R.E., ROBINSON, D. & ROWBOTHAM, G. (1991): Compositional variations in mafic phyllosilicates from regional low-grade metabasites and application of the chlorite geothermometer. *J. Metamorphic Geol.* **9**, 711-721.

BLACK, P.M. (1975): Mineralogy of New Caledonian metamorphic rocks. IV. Sheet silicates from Ouégoa District. *Contrib. Mineral. Petrol.* **49**, 269-284.

BOURQUE, P.A. (1989): Upper Ordovician to Middle Devonian rocks of Gaspé Peninsula. *In* Sedimentology, Palaeoenvironments and Palaeogeography of the Taconian to Acadian Rock Sequence of Gaspé Peninsula (P.A. Bourque, R. Hesse & B. Rust, eds.). *Geol. Assoc. Can. – Mineral. Assoc. Can., Guidebook* **B8**, 1-56.

BRINDLEY, G.W. (1961): Chlorite minerals. *In* The X-ray Identification and Crystal Structure of Clay Minerals (G.B. Brown, ed.) (2nd ed.). *Clay Mineral Group*, 242-296.

_____ & BROWN, G. (1980): Crystal Structures of Clay Minerals and their X-ray Identification. G.W. Brindley & G. Brown, eds. *Mineral. Soc., Monogr.* **5**.

_____ & GILLERY, F.H. (1956): X-ray diffraction of chlorite species. *Am. Mineral.* **41**,169-186.

BROWN, E.H. (1967): The greenschist facies in part of eastern Otago, New Zealand. *Contrib. Mineral. Petrol.* **14**, 259-292.

BROWN, G. (1955): The effect of isomorphous substitutions on the intensities of (00*l*) reflections of mica- and chlorite-type structures. *Mineral. Mag.* **30**, 657-665.

CATHELINEAU, M. (1988): Cation site occupancy in chlorites and illites as a function of temperature. *Clay Mineral.* **23**, 471-485.

_____ & NIEVA, D. (1985): A chlorite solid-solution geothermometer. The Los Azufres (Mexico) geothermal system. *Contrib. Mineral. Petrol.* **91**, 235-244.

CHAGNON, A. & DESJARDINS, M. (1991): Détermination de la composition de la chlorite par diffraction et microanalyse aux rayons X. *Can. Mineral.* **29**, 245-254.

CURTIS, C.D., IRELAND, J.B., WITHEMAN, J.A., MULVANEY, R. & WHITTLE, C.K. (1985): Authigenic chlorites: problems with chemical analysis and structural formula calculation. *Clay Mineral.* **19**, 471- 481.

DE CARITAT, P., HUTCHEON, I. & WALSHE, J.L. (1993): Chlorite geothermometry: a review. *Clays Clay Minerals* **41**, 219-239.

DUNOYER DE SEGONZAC, G. (1970): The transformation of clay minerals during diagenesis and low-grade metamorphism: a review. *Sedimentology* **15**, 281-346.

EBINA, T., IWASAKI, T., CHATTERJEE, A., KATAGIRI, M. & STUCKY, G.D. (1997): Comparative study of XPS and DFT with reference to the distributions of Al in tetrahedral and octahedral sheets of phyllosilicates. *J. Phys. Chem.* **B 101**, 1125-1129.

FOSTER, M.D. (1962): Interpretation of the composition and a classification of the chlorites. *U.S. Geol. Surv., Prof. Pap.* **414-A**.

GRIM, R.E. (1968): *Clay Mineralogy*. McGraw-Hill, New York, N.Y.

GRUNER, J.W. (1944): Composition and structure of minnesotaite, a common iron silicate in iron formations. *Am. Mineral.* **29**, 363-372.

HESSE, R. & ABID, A.I. (1998): Carbonate cementation – the key to reservoir properties of four sandstone levels (Cretaceous) in Hibernia oilfield, Jeanne d'Arc Basin, Newfoundland, Canada. *Int. Assoc. Sediment., Spec. Publ.* **26**, 363-393.

_____ & DALTON, E. (1991): Diagenetic and low grade metamorphic terrains of Gaspé Peninsula related to geologic structure of the Taconic and Acadian orogenic belts, Quebec, Appalachians. *J. Metamorphic Geol.* **9**, 775-590.

HEY, M.H. (1954): A new review of chlorites. *Mineral. Mag.* **30**, 277-292.

HILLIER, S. & VELDE, B. (1991): Octahedral occupancy and the chemical composition of diagenetic (low temperature) chlorites. *Clay Mineral.* **26**, 149-168.

INTERNATIONAL TABLES FOR X-RAY CRYSTALLOGRAPHY (1974): The Kynoch Press, Birmingham, U.K.

INTERNATIONAL TABLES FOR X-RAY CRYSTALLOGRAPHY (1992): Vol. C. Mathematical, physical and chemical tables. Wilson-Kluwer Academic Publ., Dordrecht, The Netherlands.

JOSWIG, W., FUESS, H. & MASON, S.A. (1989): Neutron diffraction study of a one-layer monoclinic chlorite. *Clays Clay Minerals* **37**, 511-514.

_____, _____, ROTHBAUER, R., TAKÉUCHI, Y. & MASON, S.A. (1980): A neutron diffraction study of a one-layer triclinic chlorite (penninite). *Am. Mineral.* **65**, 349-352.

KRANIDIOTIS, P. & MACLEAN, W.H. (1987): Systematics of chlorite alteration at the Phelps Dodge massive sulphide deposit, Matagami, Quebec. *Econ. Geol.* **82**, 1898-1911.

LAIRD, J. (1988): Chlorites: metamorphic petrology. *In* Hydrous Phyllosilicates (Exclusive of Micas) (S.W. Bailey, ed.). *Rev. Mineral.* **19**, 405-453.

MOORE, D.M. & REYNOLDS, R.C., JR. (1997): *X-Ray Diffraction and the Identification and Analysis of Clay Minerals* (2nd ed.). Oxford University Press, Oxford, U.K.

NELSON, D.O. & GUGGENHEIM, S. (1993): Infrared limitations to the oxidation of Fe in chlorite: a high-temperature single-crystal study. *Am. Mineral.* **78**, 1197-1207.

NIETO, F. (1997): Chemical composition of metapelitic chlorites – X-ray diffraction and optical property approach. *Eur. J. Mineral.* **9**, 829-841.

PETRUK, W. (1959): *The Clearwater Copper–Zinc Deposit and its Setting, with a Special Study of Mineral Zoning around such Deposits*. Ph.D. thesis, McGill Univ., Montreal, Quebec.

_____ (1964): Determination of the heavy atom content in chlorite by means of the X-ray diffractometer. *Am. Mineral.* **49**, 61-71.

PRIETO, A.C., DUBESSY, J. & CATHELINEAU, M. (1991): Structure–composition relationships in trioctahedral chlorites: a vibrational spectroscopy study. *Clays Clay Minerals* **39**, 531-539.

RADOSLOVICH, E.W. (1962): The cell dimensions and symmetry of layer-lattice silicates. II. Regression relations. *Am. Mineral.* **47**, 617-636.

RAUSELL-COLOM, J.A., WIEWIÓRA, A. & MATESANZ, E. (1991): Relationship between composition and d_{001} for chlorite. *Am. Mineral.* **76**, 1373-1379.

RUIZ CRUZ, M.D. (1997): Very low grade chlorite with anomalous chemistry and optical properties from the Malaguide complex, Betic Cordilleras, Spain. *Can. Mineral.* **35**, 923-935.

RYAN, P.C. & REYNOLDS, R.C., JR. (1997): The chemical composition of serpentine/chlorite in the Tuscaloosa Formation, United States Gulf Coast – EDX vs. XRD determination: implications for mineralogic reactions and the origin of anatase. *Clays Clay Minerals* **45**, 339-352.

SCHIFFMAN, P. & FRIDLEIFSSON, G.O. (1991): The smectite–chlorite transition in drillhole NJ–15, Nesjavellir geothermal field, Iceland: XRD, BSE and electron microprobe investigations. *J. Metamorphic Geol.* **9**, 679-696.

SCHOEN, R. (1962): Semi-quantitative analysis of chlorites by X-ray diffraction. *Am. Mineral.* **47**, 1384-1392.

SHANNON, R.D. & PREWITT, C.T. (1969): Effective ionic radii in oxides and fluorides. *Acta Crystallogr.* **B25**, 925-946.

_____ & _____ (1970): Revised values of effective ionic radii. *Acta Crystallogr.* **B26**, 1046- 1048.

SHAU, YEN-HONG & PEACOR, D.R. (1992): Phyllosilicates in hydrothermally altered basalts from DSDP Hole 504B, Leg 83 – a TEM and AEM study. *Contrib. Mineral. Petrol.* **112**, 119-133.

_____, _____ & ESSENE, E.J. (1990): Corrensite and mixed-layer chlorite/corrensite in metabasalt from northern Taiwan: TEM/AEM, EMPA, XRD, and optical studies. *Contrib. Mineral. Petrol.* **105**, 123-142.

SHIROZU, H. (1980): Cation distribution, sheet thickness, and O–OH space in trioctahedral chlorite – an X-ray and infrared study. *Mineral. J.* **10**, 14-34.

_____ & BAILEY, S.W. (1965): Chlorite polytypism. III. Crystal structure of an orthohexagonal iron chlorite. *Am. Mineral.* **50**, 868-885.

SKIDMORE, W.B. & MCGERRIGLE, H.W. (1967): Geological map of the Gaspé peninsula. *Quebec Dep. Natural Resources, Map* **1642**.

SPÖTL, C., HOUSEKNECHT, D.W. & LONGSTAFFE, F.J. (1994): Authigenic chlorites in sandstones as indicators of high-temperature diagenesis, Arkoma foreland basin, USA. *J. Sed. Res.* **A64**, 553-566.

STEINFINK, H. (1958a): The crystal structure of chlorite. I. A monoclinic polymorph. *Acta Crystallogr.* **11**, 191-195.

_____ (1958b): The crystal structure of chlorite. II. A triclinic polymorph. *Acta Crystallogr.* **11**, 195-198.

_____ (1961): Accuracy in structure analysis of layer silicates: some further comments on the structure of prochlorite. *Acta Crystallogr.* **14**, 198-199.

VELDE, B. & MEDHIOUB, M. (1988): Approach to chemical equilibrium in diagenetic chlorites. *Contrib. Mineral. Petrol.* **98**, 122-127.

WALKER, J.R. (1993): Chlorite polytype geothermometry. *Clays Clay Minerals* **41**, 260-267.

_____, HLUCHY, M.M. & REYNOLDS, R.C., JR. (1988): Estimation of heavy atom content and distribution in chlorite using corrected X-ray powder diffraction intensities. *Clays Clay Minerals* **36**, 359-364.

WALSHE, J.L. (1986): A six-component chlorite solid solution model and the conditions of chlorite formation in hydrothermal and geothermal systems. *Econ. Geol.* **81**, 681-703.

WEAVER, C.E. (1989): *Clays , Muds, and Shale*. Elsevier, Developments in Sedimentology **44**, New York, N.Y.

_____, HIGHSMITH, P.B. & WAMPLER, J.M. (1984): Chlorite. *In* Shale–Slate Metamorphism in Southern Appalachians (C.E. Weaver ed.). Elsevier, Developments in Petrology **10**, New York, N.Y. (99-139).

WHITTLE, C.K. (1986): Comparison of sedimentary chlorite compositions by X-ray diffraction and analytical TEM. *Clay Mineral.* **21**, 937-947.

WIEWIÓRA, A. & WEISS, Z. (1990): Crystallochemical classifications of phyllosilicates based on the unified system of projection of chemical composition. II. The chlorite group. *Clay Mineral.* **25**, 83- 92.

XIE, XIAOGANG, BYERLY, G.R. & FERRELL, R.E., JR. (1997): IIb trioctahedral chlorite from the Barberton greenstone belt: crystal structure and rock composition constraints with implications to geothermometry. *Contrib. Mineral. Petrol.* **126**, 275-291.

Received February 8, 1998, revised manuscript accepted December 15, 1998.

APPENDIX: PROGRAM CALCULATION AND THEORETICAL BACKGROUND

This user-friendly program contains two spreadsheets that run on the Excel program, version 7. The program makes use of the different scattering power of the heavy and light cations in octahedrally coordinated sites. The heavy atoms Fe, Mn, Cr, Ni have greater scattering power than the light atoms Mg and Al (as recorded by the X-ray intensities of basal reflections at low-2θ angles). The input data that are required are the intensities of the first five basal reflections as well as the *d*-values of the third and fifth basal reflections of chlorite. The asymmetry is calculated on the first spreadsheet called "Input-sy.xls", *via* construction of the curve that relates *F*(003)/*F*(005) and (D). Total [Fe] content is calculated with the second spreadsheet called "Str-chl.xls". The ratio [*F*(002) + *F*(004)]/*F*(003) was used to determine the total [Fe] content after making allowance for the effect of asymmetry on I(003).

The input data are pasted on the first sheet (input-sy.xls). Choosing the "copy" command of the edit menu in the user spreadsheet does this. Paste special "values only" on the Input-sy.xls sheet. The actual data begin in cell B3. The *d*(060) reflection must be recorded to check whether the mineral is dioctahedral or trioctahedral. In the latter case, the next step is to calculate [Si], [^{IV}Al], and [^{VI}Al] using the *d*(003) and *d*(005) values from the Input-sy.xls spreadsheet as outlined in the main text (equations. 1 and 2). The resultant values of [Si], [^{IV}Al], and [^{VI}Al] are then used to calculate *F*, the structure-factor values, according to:

$$F = N f_a \cos 2\theta\, lz \qquad \text{(Eq. 5)}$$

where *N* is the number of atoms or ions per unit cell, f_a is the mean scattering factor value for chemically significant ions, *l* is an integer denoting the order of the basal reflection, and *z* is the fractional coordinate of the atom normal to the (001) reflection.

The values of *N* [O] and [OH] are fixed all over the two spreadsheets (Input-sy.xls and Str-chl.xls), whereas [Fe] is predetermined in a schematic way to cover all the possibilities of asymmetry. [Si], [^{IV}Al] and [^{VI}Al] are automatically transferred from the calculations using equations 1 and 2 to the spreadsheet, whereas [Mg] is determined from the total number of cations in the sheet of octahedra, taking into consideration the possibility of vacancies. Then these data are pasted to the proper cell for structure-factor calculations.

For the scattering factors of the atoms in planes containing O, OH and H ions, only the O atoms are counted; OH-groups and H ions are ignored. Values of the scattering factors are variable according to the wavelength of the radiation used, and the 2θ of the basal reflection.

The *z* fractional coordinates of the chlorite-group minerals are those published by Joswig *et al.* (1980, 1989) and Steinfink (1958a, b, 1961), who refined the structure of both triclinic and monoclinic polymorphs using single-crystal diffraction data. These data are customarily used as the distance of atoms from the center of symmetry measured along a line normal to the (00l) plane.

After construction of the diagram that relates the asymmetry in the distribution of Fe to the ratio *F*(003)/*F*(005) (logarithmic relationship of Fig. 3), the measured intensity data are converted to structural factors according to

$$I = |F|^2 L_p F \qquad \text{Eq. (6),}$$

where F is the interference function, which carries information on crystallite size and strain (Moore & Reynolds 1997). The details of the calculation of L_p and F are given in spreadsheet "Input-sy.xls".

In the next step, the program compares the measured *F*(003)/*F*(005) values with the theoretical *F*(003)/*F*(005) values in order to derive the asymmetry value. In other words, the asymmetry values are obtained from the trend of the theoretical curve. Note that this theoretical curve is very close to the real value, hence the [Si], [^{IV}Al] and [^{VI}Al] are actually deduced from the measured values. All these data are transferred automatically to the second spreadsheet (Str-chl.xls). Moreover, the correction of the *I*(003) value due to the asymmetrical distribution of Fe in octahedral sites is calculated using Eq. (4). One can move from Input-sy.xls to Str-chl.xls by clicking on the tabs in the lower left corner of the spreadsheet. Check the associated curves to verify that all F or I values are positive numbers; do not include negative values.

On the Str-chl.xls sheet, the structural values of the even reflections are calculated. Next, the curve that relates [*I*(002) + *I*(004)]/$I(003)_{C^*}$ to total [Fe] is constructed [after correction of the *I*(003) value for asymmetry]. The trend of the curve is always a polynomial of the third order (Fig. 3).

It is always necessary to check the curve because the calculation of *N*, for example for [Mg], may yield a negative value, which has no physical meaning and will disturb the construction of the curve. Negative values are skipped by proceding to the next data point.

Structural formulae of chlorite-group minerals are calculated based on 28 oxygen equivalents (56 negative charges), *i.e.*, assuming an ideal anion framework of $O_{20}(OH)_{16}$, with the total (O + OH) = 36, total positive charges = 56, and total number of cations = 20. The calculations in the program are carried out under the assumption that total Fe varies from 0 to 6, and Fe asymmetry between +3.0 and –3.0. These limits appear to be sufficient for common chlorites, but the program extrapolates beyond these ranges, if required.